# A NEW APPROACH TO OVERCOME THE OVERFLOW PROBLEM IN COMPUTER-AIDED ANALYSIS OF NONLINEAR RESISTIVE CIRCUITS

by

Leon O. Chua and Niantsu N. Wang

Memorandum No. ERL-M470

6 September 1974

ELECTRONICS RESEARCH LABORATORY

College of Engineering
University of California, Berkeley
94720

# A NEW APPROACH TO OVERCOME THE OVERFLOW PROBLEM IN COMPUTER-AIDED ANALYSIS OF NONLINEAR RESISTIVE CIRCUITS

Leon O. Chua and Niantsu N. Wang

Department of Electrical Engineering and Computer Sciences
and the Electronics Research Laboratory
University of California, Berkeley, California 94720

## ABSTRACT

This paper is addressed to the so-called overflow problem commonly encountered in the computer simulation of nonlinear resistive circuits containing rapidly varying nonlinearities -- such as exponentials found in the models of diodes and transistors. A novel approach which makes use of the arc-lengths of the nonlinear characteristic curves as the variables of iteration is proposed. It is proved, under rather mild conditions, that the arc-length approach not only overcomes the overflow problem, but also leads to a more rapid rate of convergence. Moreover, it is proved that for most practical diode-transistor circuits, the region of convergence associated with the arc-length approach enlarges rapidly as the number of diodes and transistors increases. Hence in so far as choosing the initial guess is concerned, the advantage for using the arc-length approach over the conventional approach increases with the size of the network. Extensive numerical experiments confirm the superior convergence property of this approach even for circuits which violate the sufficient conditions invoked by the rigorous mathematical proofs.

---

Research sponsored by the U.S. Navy Electronic System Command, Contract N00039-71-C-0255 and NSF Grant GK-32236X1

Although the approach is applicable to a much wider class of nonlinear networks, particular emphasis is focused on diode-transistor networks in this paper.

## I. INTRODUCTION

The overflow problem often encountered in computer-aided transistor circuit analysis is best illustrated by considering the simple diode circuit shown in Fig. 1 (a). The diode is characterized by the equation

$$i = I_s(e^{v/V_T} - 1) \triangleq \hat{i}(v) \tag{1}$$

where typically the saturation current $I_s \cong 10^{-13}$ A and the thermal voltage $V_T \triangleq kT/q$ is approximately 0.026 V at room temperature. The network equation of the circuit is given by

$$f(v) \triangleq \hat{i}(v) + \frac{1}{R}v - \frac{E}{R} = 0 \tag{2}$$

and the Newton-Raphson algorithm for solving (2) is:

$$v^{k+1} = v^k - \frac{f(v^k)}{f'(v^k)} \tag{3}$$

$$k = 0, 1, 2, \ldots$$

where $f'(v^k) \triangleq df(v^k)/dv$; $v^k$ being the k-th iterate, and in particular, $v^0$ is the initial guess. Convergence property of (3) depends heavily on the initial guess $v^0$. A clever choice of $v^0$ can affect the rate of convergence significantly. On the other hand, since $V_T$ is very small, $e^{v/V_T}$ increases rapidly with v. For v > 19 V, $\hat{i}(v)$ is extremely large and overflow problems occur in evaluating (3) on most computers. In table 1[1] we summarized the rates of convergence corresponding to different values of E and R. For comparison, we always started at $v^0 = 0$ V. As shown in column 4 of the table, convergence became extremely slow for large values of E and small values of R. For E > 15 V and R < 1 Ohm,

for example, the Newton-Raphson algorithm fails due to overflow. Several approaches have been proposed to overcome this problem:

(1) Source Stepping ([1]). We start from a particular input with a known solution and then change the input step by step toward the desired input. At each step we compute the solution using the solution corresponding to the previous input as the initial guess. Finding a proper step size at each cycle is a fairly difficult problem and the whole process is very time-consuming.

(2) Step-Size Modification ([2], [3]). At each iteration we introduce an appropriate step-size factor $\lambda^k > 0$ into (3); namely,

$$v^{k+1} = v^k - \lambda^k \frac{f(v^k)}{f'(v^k)}$$

The value of $\lambda^k$ is usually chosen by some intricate scheme in order to keep $v^{k+1}$ within some reasonable range. This method has severe drawbacks. First of all, since the main purpose of this approach is to guarantee the convergence of the algorithm, the value of $\lambda^k$ needed for overcoming overflow may not be desirable for guaranteeing convergence. Secondly, the schemes for computing an appropriate $\lambda^k$ are rather time-consuming.

(3) Voltage-Current Switching. Since $|dv/di|$ is small whenever $|di/dv|$ is large, this approach suggests repetitive switching between voltages and currents as the independent variables. Unfortunately, the convergence of this approach is questionable.

(4) Pre-set Bounds ([4], [5]). Since one often has some idea of the magnitudes of v and i associated with practical circuits, this approach consists of setting a-priori bounds for them. Whenever the computed $v^k$

[1] All numerical examples in this paper are obtained from the CDC 6400 computer.

exceeds this bound, a new value is chosen. Not only is the effect of this approach on convergence extremely difficult to establish, it also defeats partly the purpose of computing the derivatives.

As we have seen the preceding approaches are computationally inefficient and are ad hoc in nature in the sense that they often work only for some special class of problems. To overcome the preceding objections, a novel approach using the arc-lengths of the v - i curves as the variables to be solved is proposed in this paper. For example, as will be shown in Section III, the diode characteristic can be described by $v = \hat{v}(\rho)$ and $i = \hat{i}(\rho)$ where $\rho$ is the arc-length of the v - i curve starting from the point v = i = 0. For comparison, the functions $\hat{i}(v)$, $\hat{i}(\rho)$ and $\hat{v}(\rho)$ for the diode are shown in Fig. 2 along with their derivatives. In terms of the arc-length $\rho$, (2) and (3) become

$$f(\rho) = \hat{i}(\rho) + \frac{1}{R}\hat{v}(\rho) - \frac{E}{R} = 0 \tag{4}$$

and

$$\rho^{k+1} = \rho^k - \frac{f(\rho^k)}{f'(\rho^k)} \qquad k = 0, 1, 2, \ldots \tag{5}$$

respectively. Notice that since both $|d\hat{i}/d\rho| < 1$ and $|d\hat{v}/d\rho| < 1$ in Fig. 2, the function $f(\rho)$ satisfies a global Lipschitz condition and (5) converges much faster than (3). Moreover, the overflow problem never occurs here. The superior convergence property of this approach can be seen by comparing the last two columns of Table 1.

Table 1. Comparison of the rate of convergence of the Newton-Raphson algorithm with "diode voltage" and "arc-length" as the respective variables of iteration. Precision: 8 digits after the decimal point.

| E (V) | R (ohms) | v (V) | Iterations on voltage | Iterations on arc-length |
|---|---|---|---|---|
| 1 | 1 | .84887700 | 12 | 4 |
| 1 | $10^3$ | .68811353 | 18 | 10 |
| 2 | 1 | .90047502 | 49 | 4 |
| 10 | .1 | 1.0149600 | over 250 | 5 |

For comparison, we plot both $f(v)$ and $f(\rho)$ in Figs. 1 (b) and (c) corresponding to E = 2 V and R = 1 ohm. For arc-length approach the iterates $\{\rho^k\}$ almost hit the solution in one step.

To prove that the preceding desirable properties associated with the arc-length interation are true for a large class of nonlinear circuits, we carry out an analysis of the network equations in terms of arc-lengths in Sections II and III. In Section IV we investigate properties of the Jacobian matrices associated with the Newton-Raphson algorithm applied to network equations. The formal proof that our approach overcomes overflow problem is given in Section V under rather general settings. The superior convergence property of the arc-length approach is established in Section VI for the Newton-Raphson algorithm. Finally, the assertions in the preceding sections are illustrated by several examples in Section VII. It must be emphasized that the arc-length approach, though particularly suited to diode nonlinearities, is useful for analyzing any network containing resistors characterized by

v - i curves with rapidly-varying nonlinearities.

Finally, some remarks concerning notations: (1) We use lower-case letters with subscripts for components of vectors. Thus $v = (v_1, v_2, \ldots, v_n)^t \in \mathbb{R}^n$; where t means transposition. All vectors are defined to be column vectors. We use upper-case letters for matrices in $\mathbb{R}^{n \times n}$. (2) Functions are denoted by "hats", thus $v = \hat{v}(i)$ means that the variable v is computed via the function $\hat{v}(\cdot)$ at i. (3) Since we shall use hybrid analysis to describe circuits, we use E and I to denote the sets of indices pertaining to voltage ports and current ports, respectively. Thus $i_k$, $k \in E$ means the current associated with the "voltage port" k. (4) Finally, we define two kinds of norms. Let $z = (z_1, \ldots, z_n)^t \in \mathbb{R}^n$. The $\ell_1$-norm of z denoted by $\|z\|$, is defined as $\|z\| = \sum_{i=1}^{n} |z_i|$. The $\ell_\infty$ - norm of z, denoted by $\|z\|_\infty$, is defined as $\|z\|_\infty = \max_i \{|z_i|, i = 1, 2, \ldots, n\}$. Let $A \triangleq [a_{ij}] \in \mathbb{R}^{n \times n}$. The induced $\ell_1$-norm and $\ell_\infty$-norm of A are denoted by $\|A\|$ and $\|A\|_\infty$, respectively. It is well known that $\|A\| = \max_j \sum_{i=1}^{n} |a_{ij}|$ and $\|A\|_\infty = \max_i \sum_{j=1}^{n} |a_{ij}|$. Hence, $\|A\| = \|A^t\|_\infty$.

## II. EQUATION FORMULATION VIA HYBRID ANALYSIS

Throughout this paper we use hybrid analysis to formulate the network equations by extracting all nonlinear resistors and replacing them by voltage and/or current ports, as shown in Fig. 3 (a). The remaining n-port, which contains only linear resistors, linear controlled sources and independent sources, is then described by a hybrid representation. Not only is hybrid analysis particularly suited to the arc-

length approach but it also offers many advantages over the more widely used nodal analysis; namely, (1) hybrid analysis can be applied to circuits containing both voltage-controlled and current-controlled elements, (2) hybrid analysis can handle all four types of linear controlled sources while nodal analysis, strictly speaking, allows only voltage-controlled current-sources, (3) for circuits containing relatively few nonlinear resistors, the system of nonlinear network equations obtained by hybrid analysis is of a much lower dimension than that obtained by nodal analysis, (4) in many cases, hybrid analysis provides the most convenient formulation for investigating theoretical properties, such as the existence and the uniqueness of solutions, of network equations.

In the following, we describe the hybrid formulation briefly and state some important properties. For detailed discussions, see [6], [7], and [9].

Theorem 1. ([9])

A linear n-port $\mathcal{N}$ containing only positive linear resistors has a hybrid representation

$$\begin{bmatrix} i_E \\ v_I \end{bmatrix} = -\begin{bmatrix} H_{EE} & H_{EI} \\ H_{IE} & H_{II} \end{bmatrix} \begin{bmatrix} v_E \\ i_I \end{bmatrix}, \tag{6}$$

where E and I pertain to voltage ports and current ports, respectively, if and only if the voltage ports do not form any loops and the current ports do not form any cut sets.

The negative sign associated with the hybrid matrix in Eq. (6) is due to the reference sign convention shown in Fig. 3 (a). We state a few important properties of the submatrices in Eq. (6):

P1. $H_{EI} = -H_{IE}^t$ .

P2. $H_{EE}$ and $H_{II}$ are real symmetric, positive semidefinite or positive definite. Nullity of $H_{EE}$ (resp. $H_{II}$) is equal to the number of independent cut sets (resp. loops) consisting of voltage and/or current ports only.

P3. Elements of $H_{EI}$ and $H_{IE}$ are bounded by 1 in magnitude.

P4. Let $H \triangleq \begin{bmatrix} H_{EE} & H_{EI} \\ H_{IE} & H_{II} \end{bmatrix}$, since $H + H^t = \begin{bmatrix} 2H_{EE} & 0 \\ 0 & 2H_{II} \end{bmatrix}$, H is at least positive semidefinite. It is positive definite if and only if both $H_{EE}$ and $H_{II}$ are positive definite. In particular, H is positive definite and hence is nonsingular if the voltage ports and the current ports do not form any loops or cut sets. Otherwise H is singular.

In the general case where the n-port contains also linear controlled sources and independent sources, under some mild conditions, the following hybrid representation can be generated efficiently by topological methods [6]:

$$\begin{bmatrix} i_E \\ v_I \end{bmatrix} + H \begin{bmatrix} v_E \\ i_I \end{bmatrix} = s \qquad (7)$$

where H is of the form defined in (6) and the source vector s accounts for the independent sources. If there are no controlled sources inside the n-port, H satisfies all properties P1 - P4, otherwise it is arbitrary. The port voltages and currents are related by the v - i characteristics of the nonlinear resistors:

$$i_E = \hat{i}_E(v_E) \quad \text{and} \quad v_I = \hat{v}_I(i_I) \qquad (8)$$

Notice that both $\hat{i}_E(\cdot)$ and $\hat{v}_I(\cdot)$ are <u>diagonal functions</u>, i.e., $i_k = \hat{i}_k(v_k)$ is a function of $v_k$ only. From (7) and (8) we obtain

$$f(v_E, i_I) \triangleq \begin{bmatrix} \hat{i}_E\ (v_E) \\ \hat{v}_I\ (i_I) \end{bmatrix} + H \begin{bmatrix} v_E \\ i_I \end{bmatrix} - s = 0 . \qquad (9)$$

Equation (9) can be solved by many iterative methods, including the Newton-Raphson method to be investigated in detail in subsequent sections. Before we consider the solution of (9), however, let us investigate two important special cases associated with diode-transistor networks.

Special Case 1.

Consider a circuit containing diodes, transistors, positive linear resistors and independent sources. Replace each transistor by its Ebers-Moll model as shown in Fig. 4 (b). Extracting all diodes as voltage and/or current ports, and imbedding the linear controlled sources within the n-port $\mathcal{N}$, we obtain a hybrid representation given by (9). Notice again that $\hat{i}_E(\cdot)$ and $\hat{v}_I(\cdot)$ are diagonal, i.e., $i_k = \hat{i}(v_k)$, $k \in E$ and $v_m = \hat{v}(i_m)$, $m \in I$, where $\hat{i}(\cdot)$ is defined by (1) and $\hat{v}(\cdot) = \hat{i}^{-1}(\cdot)$ whenever the inverse exists.

Special Case 2.

Consider the same circuit in Special Case 1 but with no diodes[2]. Extract each "diode-controlled source combination" as a voltage port as shown in Fig. 4 (c). Suppose the hybrid representation[3] exists so that we have

$$\hat{i}_E(v_E) + G'\ v_E - s = 0$$

---

[2] We exclude the diodes just for simplicity. In fact, each diode will add only a "1" along the diagonal of the matrix T defined below.

[3] In this case, it is the usual admittance representation of the associated n-port. Hence, in case 2, we will use the symbols G and G' to denote the short-circuit admittance matrix associated with the two n-ports $\mathcal{N}$ in Fig. 3 (a) and $\mathcal{N}'$ in Fig. 3 (b), respectively.

where the components of $\hat{i}_E(\cdot)$ are defined by (see Fig. 4 (c))

$i_k = \hat{i}(v_k) - \alpha_F\, \hat{i}(v_{K+1})$ and $i_{k+1} = \hat{i}(v_{k+1}) - \alpha_R\, \hat{i}(v_k)$ etc.,

$k = 1, 3, 5, \ldots, n/2$. Notice that in this case $\hat{i}_E(\cdot)$ is no longer diagonal. However, since there are no controlled sources inside the n-port, $\eta'$, matrix G' possesses all properties P1 - P4. Let G be the corresponding admittance matrix obtained by the method described in Special Case 1, it is obvious that

$$G = T^{-1}\, G'$$

where

$$T = \begin{bmatrix} 1 & -\alpha_F & & & & \\ -\alpha_R & 1 & & & & \\ & & 1 & -\alpha_F & & \\ & & -\alpha_R & 1 & & \\ & & & & 1 & -\alpha_F \\ & & & & -\alpha_R & 1 \end{bmatrix}$$

Although we will not use this model for computation, the relation $G = T^{-1}\, G'$ is useful for investigating properties of G. For example, G is nonsingular whenever G' is, and the singularity of G' can readily be checked by inspection of the associated network topology (see property P2). A circuit with its transistors replaced by this model is shown in Fig. 3 (b). Notice that $\eta'$ does not contain any controlled sources.

## III. PARAMETRIC REPRESENTATION -- THE ARC-LENGTH APPROACH

A curve in the v - i plane can be represented parametrically by

$$v = \hat{v}(\rho) \text{ and } i = \hat{i}(\rho)$$

where $\rho$ is called a parameter. In case the v - i curve is rectifiable [11];

a condition satisfied by all v - i curves of practical interest, $\rho$ can be chosen as the arc-length of the curve measured from an arbitrary point on the curve to the point (v, i). Observe that the parametric representation remains applicable even if the v - i curve of a resistor is neither voltage- nor current-controlled. In the following, we derive a few useful properties of this representation:

(1) $\left(\frac{d\hat{i}}{d\rho}\right)^2 + \left(\frac{d\hat{v}}{d\rho}\right)^2 = 1$, whenever the derivatives exist. (10)

Moreover, $|d\hat{i}/d\rho| \leq 1$ and $|d\hat{v}/d\rho| \leq 1$ for all $\rho \in R$.

Proof. Since $(d\rho)^2 = (di)^2 + (dv)^2$, (10) follows.

(2) A curve is completely specified by only one parametric equation and one point $(v_0, i_0)$ on the curve.

Proof. From (10), we have

$$i(\rho) = \int_0^{\rho} \sqrt{1 - \left(\frac{dv}{d\rho'}\right)^2}\, d\rho' + i_0 \quad \text{and} \quad v(\rho) = \int_0^{\rho} \sqrt{1 - \left(\frac{d\hat{i}}{d\rho'}\right)^2}\, d\rho' + v_0.$$

(3) The arc-length $\rho$ can be computed by either

$$\rho(i) = \int_{i_0}^{i} \sqrt{1 + \left(\frac{d\hat{v}}{di'}\right)^2}\, di' \quad \text{or} \quad \rho(v) = \int_{v_0}^{v} \sqrt{1 + \left(\frac{d\hat{i}}{dv'}\right)^2}\, dv' \quad (11)$$

Proof. Obvious from (10).

(4) Let $d\hat{i}/dv \triangleq x$, then

$$\left|\frac{d\hat{i}}{d\rho}\right| = \frac{|x|}{\sqrt{1 + x^2}}, \quad \left|\frac{d\hat{v}}{d\rho}\right| = \frac{1}{\sqrt{1 + x^2}} \quad (12)$$

and if the v-i curve is monotonically increasing, we have

$$\frac{d^2\hat{i}}{d\rho^2} = \frac{1}{(1 + x^2)^2}\left(\frac{d^2\hat{i}}{dv^2}\right), \quad \frac{d^2\hat{v}}{d\rho^2} = -\frac{x}{(1 + x^2)^2}\left(\frac{d^2\hat{i}}{dv^2}\right) \quad (13)$$

Proof. By direct computation.

(5) If we define $x \triangleq d\hat{v}/di$, property (4) is still true with v and i interchanged.

To illustrate the arc-length approach, consider a diode characterized by (1). Since the v - i curve passes through the origin, it is convenient to choose $(v_0, i_0) = (0, 0)$. By (11)

$$\rho(v) = \int_0^v \sqrt{1 + \left(\frac{d\hat{i}}{dv'}\right)^2}\, dv' = \int_0^v \sqrt{1 + \theta^2\, e^{2v'/V_T}}\, dv'$$

where $\theta \triangleq I_s/V_T$. Since $x \triangleq d\hat{i}/dv = \theta\, e^{v/V_T}$, we have[4]

$$\boxed{\rho = V_T\left\{\log\left(\frac{1}{1 + \sqrt{1 + x^2}}\right) + \sqrt{1 + x^2}\right\} + c_1} \qquad (14)$$

where $c_1 \triangleq -V_T\left\{\log\left(\frac{\theta}{1 + \sqrt{1 + \theta^2}}\right) + \sqrt{1 + \theta^2}\right\}$ is a constant.

Equation (14) defines x as an implicit function of ρ. Given ρ, we solve for x from (14) and then obtain v and i from

$$\boxed{v(x) = V_T \log(x/\theta) \quad \text{and} \quad i(x) = V_T\, x - I_s\ .} \qquad (15)$$

Notice that since the v - i curve is strictly monotonically increasing, $x \in (0,\infty)$ and the right-hand side of (14) is a concave function of x. Hence, for each ρ, there exists a unique solution $x(\rho)$. The Newton-Raphson iteration applied to (14) converges rapidly for small initial guesses $x^0$. In practice, we may simply assume different values of ρ and have the functions $v = \hat{v}(\rho)$ and $i = \hat{i}(\rho)$ tabulated and stored in the computer in the same way that a v - i curve may be stored as a table of points. This can be done easily because $i(\rho) \cong \rho$ for large ρ

---

[4] See Appendix A1 for the derivation.

and $v(\rho) \tilde{=} \rho$ for small $\rho$. The same table, with a simple modification, can be used for different values of $V_T$ corresponding to different temperatures. (See Appendix A2 for details.) Let us now consider two examples.

Example 1.

Consider the class of circuits belonging to Special Case 1 of Section II. If we use the arc-lengths $\rho$ as independent variables, we have from (9)

$$f(\rho_E, \rho_I) \triangleq \begin{bmatrix} \hat{i}_E(\rho_E) \\ \hat{v}_I(\rho_I) \end{bmatrix} + H \begin{bmatrix} \hat{v}_E(\rho_E) \\ \hat{i}_I(\rho_I) \end{bmatrix} - s = 0. \qquad (16)$$

where $i_k = \hat{i}(\rho_k)$ and $v_k = \hat{v}(\rho_k)$, $k \in E \cup I$. The functions $\hat{i}(\cdot)$ and $\hat{v}(\cdot)$ are defined by (14) and (15). See Fig. 4 (d).

Example 2.

Consider the same representation as in Special Case 2 of Section II. In this case we have $i_k = \hat{i}_k(\rho_k, \rho_{k+1}) \triangleq \hat{i}(\rho_k) - \alpha_F \hat{i}(\rho_{k+1})$ and $i_{k+1} = \hat{i}_{k+1}(\rho_k, \rho_{k+1}) \triangleq \hat{i}(\rho_{k+1}) - \alpha_R \hat{i}(\rho_k)$, etc. See Fig. 4 (e).

## IV. PROPERTIES OF THE JACOBIAN MATRIX ASSOCIATED WITH THE NEWTON-RAPHSON ALGORITHM

Let us now investigate and compare the solution of the network equations given by (9) and (16) by the Newton-Raphson method. Let f be a function from $\mathbb{R}^n$ into $\mathbb{R}^n$, find a $z^* \in \mathbb{R}^n$ such that $f(z^*) = 0$. The successive iterates are computed by

$$z^{k+1} = z^k - J_z^{-1}(z^k) f(z^k), \quad k = 0, 1, 2, \ldots \qquad (17)$$

where $J_z(z^k) \triangleq \partial f(z^k)/\partial z$ is the Jacobian matrix of f and $z^0$ is the initial guess. Applying (17) to (9), we have

$$\begin{bmatrix} v_E \\ i_I \end{bmatrix}^{k+1} = \begin{bmatrix} v_E \\ i_I \end{bmatrix}^{k} - [J_{v,i}^{(k)}]^{-1} f(v_E, i_I)^k \qquad (18)$$

$$k = 0, 1, 2, \ldots$$

where

$$J_{v,i} \triangleq \frac{\partial f(v_E, i_I)}{\partial(v_E, i_I)} = \begin{bmatrix} \frac{d\hat{i}_1}{dv_1} & & & 0 & \\ & \ddots & & & \\ & & \frac{d\hat{i}_m}{dv_m} & & \\ & 0 & & \frac{d\hat{v}_{m+1}}{di_{m+1}} & \\ & & & & \ddots \\ & & & & \frac{d\hat{v}_n}{di_n} \end{bmatrix} + H \triangleq D(v_E, i_I) + H \qquad (19)$$

where D is a diagonal matrix because $\hat{v}_E(\cdot)$ and $\hat{i}_I(\cdot)$ are diagonal functions. Here $E = \{1, 2, \ldots m\}$ and $I = \{m + 1, m + 2, \ldots n\}$ .

Applying (17) to (16), we obtain

$$\begin{bmatrix} \rho_E \\ \rho_I \end{bmatrix}^{k+1} = \begin{bmatrix} \rho_E \\ \rho_I \end{bmatrix}^{k} - [J_\rho^{(k)}]^{-1} f(\rho_E, \rho_I)^k \qquad (20)$$

where

$$J_\rho \triangleq \frac{\partial f(\rho_E, \rho_I)}{\partial(\rho_E, \rho_I)} = \begin{bmatrix} \frac{d\hat{i}_1}{d\rho_1} & & & & \\ & \ddots & & & \\ & & \frac{d\hat{i}_m}{d\rho_m} & & \\ & & & \frac{d\hat{v}_{m+1}}{d\rho_{m+1}} & \\ & & & & \ddots \\ & & & & \frac{d\hat{v}_n}{d\rho_n} \end{bmatrix} + H \begin{bmatrix} \frac{d\hat{v}_1}{d\rho_1} & & & & \\ & \ddots & & & \\ & & \frac{d\hat{v}_m}{d\rho_m} & & \\ & & & \frac{d\hat{i}_{m+1}}{d\rho_{m+1}} & \\ & & & & \ddots \\ & & & & \frac{d\hat{i}_n}{d\rho_n} \end{bmatrix}$$

$$\triangleq D_1(\rho_E, \rho_I) + H\, D_2(\rho_E, \rho_I). \qquad (21)$$

Whether the sequences defined by (18) and (20) converge depends on both the initial guess and the behavior of the Jacobian matrix. For example, the sequence will not converge if the Jacobian matrix becomes singular at some k. In this section we establish a few important properties of the Jacobian matrix.

(1) Bounds for $J_\rho$

Theorem 2. Let N be a circuit characterized by the hybrid equation (16). Then $J_\rho$ is bounded by

$$\|J_\rho\| \leq \sqrt{\|H\|^2 + 1} \tag{22}$$

Proof. Let $H = [h_{ij}]$ in (16). Then the j-th column vector $J_\rho^j$ of $J_\rho$ is given by

$$J_\rho^j = [h_{1j} \frac{d\hat{v}_j}{d\rho_j}, \cdots \frac{d\hat{i}_j}{d\rho_j} + h_{jj} \frac{d\hat{v}_j}{d\rho_j}, \cdots h_{nj} \frac{d\hat{v}_j}{d\rho_j}]^t, \quad j \in E$$

and

$$J_\rho^j = [h_{1j} \frac{d\hat{i}_j}{d\rho_j}, \cdots \frac{d\hat{v}_j}{d\rho_j} + h_{jj} \frac{d\hat{i}_j}{d\rho_j}, \cdots h_{nj} \frac{d\hat{i}_j}{d\rho_j}]^t, \quad j \in I.$$

To be specific, let $j \in E$ we have

$$\begin{aligned} \|J_\rho^j\| &= \Big(\sum_{\substack{k=1 \\ k\neq j}}^{n} |h_{kj}|\Big)\Big|\frac{d\hat{v}_j}{d\rho_j}\Big| + \Big|\frac{d\hat{i}_j}{d\rho_j} + h_{jj}\frac{d\hat{v}_j}{d\rho_j}\Big| \\ &\leq \Big|\frac{d\hat{i}_j}{d\rho_j}\Big| + \Big(\sum_{k=1}^{n} |h_{kj}|\Big)\Big|\frac{d\hat{v}_j}{d\rho_j}\Big| \\ &\leq \Big|\frac{d\hat{i}_j}{d\rho_j}\Big| + \|H\| \cdot \Big|\frac{d\hat{v}_j}{d\rho_j}\Big| \end{aligned}$$

Since, $(d\hat{i}/d\rho)^2 + (d\hat{v}/d\rho)^2 = 1$, let $|d\hat{i}_j/d\rho_j| = \cos\theta_j$ and $|d\hat{v}_j/d\rho_j| = \sin\theta_j$ where $\theta_j \in [0, \pi/2]$. Hence we have

$$\|J_\rho^j\| \leq \cos\theta_j + \|H\| \sin\theta_j \qquad \theta_j \in [0, \pi/2].$$

It then follows from Appendix A3 that

$$\|J_\rho^j\| \leq \sqrt{\|H\|^2 + 1}\ , \quad j \in E.$$

Similarly, $\|J_\rho^j\| \leq \sqrt{\|H\|^2 + 1}$, $j \in I$. This proves that $\|J_\rho\| \leq \sqrt{\|H\|^2 + 1}$ . □

Corollary. Consider the same circuit as in Theorem 2. Assume that (i) $h_{jj} \geq 0$ for all $j \in E \cup I$, (ii) all nonlinear resistors are monotonically increasing, then

$$\min_j \{\|H^j\|, 1\} \leq \|J_\rho\|.$$

where $H^j$ denotes the j-th column vector of H.

Proof. Since all nonlinear resistors are monotonically increasing, $d\hat{i}_j/d\rho_j \geq 0$ and $d\hat{v}_j/d\rho_j \geq 0$ for all $j \in E \cup I$. Then $\|J_\rho^j\| = (d\hat{i}_j/d\rho_j) + \|H^j\|\,(d\hat{v}_j/d\rho_j)$, $j \in E$ and $\|J_\rho^j\| = (d\hat{v}_j/d\rho_j) + \|H^j\|\,(d\hat{i}_j/d\rho_j)$, $j \in I$. By Appendix A3, $\|J_\rho^j\| \geq \min\{\|H^j\|, 1\}$ $j \in E \cup I$. □

(2) Singularly of the Jacobian Matrix

In applying the Newton-Raphson method, we must ensure that the Jacobian matrices are nonsingular. Since

$$J_\rho(\rho_E, \rho_I) = J_{v,i}\,(v_E, i_I)\,\frac{\partial(v_E, i_I)}{\partial(\rho_E, \rho_I)}$$

$J_\rho$ is nonsingular if both $J_{v,i}$ and $\partial(v_E, i_I)/\partial(\rho_E, \rho_I)$ are finite and nonsingular. This is, however, not the only case. $J_\rho$ can be nonsingular even if $\partial(v_E, i_I)/\partial(\rho_E, \rho_I)$ is singular as can be seen from the equation $dv/d\rho = (dv/di)(di/d\rho)$. Observe that $di/d\rho = 0$ implies $dv/d\rho = 1$. In many practical cases, for example, transistor circuits, where all non-

linear resistors are strictly monotonically increasing, the associated matrix $\partial(v_E, i_I)/\partial(\rho_E, \rho_I)$ is always nonsingular. In this case, the singular points of $J_{v,i}$ and $J_\rho$ are in one-to-one correspondence and the following theorem gives a sufficient condition which ensures that $J_\rho$ is non-singular.

Theorem 3. Consider a circuit described by (9) and the associated Newton-Raphson iteration given by (18). Assume H is nonsingular. Then $J_{v,i}(v_E, i_I)$ is nonsingular if $\|H^{-1}\| \cdot \max \{|di_k/dv_k|, |dv_m/di_m|; k \in E, m \in I\} < 1$.

Proof. From (19), $J_{v,i}(v_E, i_I) = D(v_E, i_I) + H = H(1 + H^{-1} D(v_E, i_I))$. Since $\|D(v_E, i_I)\| = \max \{|d\hat{i}_k/dv_k|, |d\hat{v}_m/di_m|; k \in E, m \in I\}$ and $J_{v,i}(v_E, i_I)$ is nonsingular if $\|H^{-1}\| \cdot \|D(v_E, i_I)\| < 1$,[5] the theorem follows. □

Remark. In view of Theorem 3, $J_{v,i}$ is nonsingular if $\|D(v_E, i_I)\|$ is sufficiently small. This means that $|di_k/dv_k|$ should be small for voltage ports and $|dv_m/di_m|$ should be small for current ports. For example, if we know the bias polarities of some transistors, which is usually the case for many practical transistor circuits, then it is desirable to choose forward biased branches as current ports and reverse biased branches as voltage ports.

Theorem 4. Consider a circuit characterized by (9). Assume that (i) there are no controlled sources in the circuit; (ii) the nonlinear resistors do not form any loops or cut sets; (iii) all nonlinear resistors are monotonically increasing, then the Jacobian matrix $J_{v,i}(v_E, i_I)$ defined by (19) is nonsingular for all $(v_E, i_I) \in \mathbb{R}^n$.

---

[5] The matrix (I + A) is nonsingular if $\|A\| < 1$, see [10].

Proof. By (i), $H_{IE} = -H_{EI}^t$; by (ii), both $H_{EE}$ and $H_{II}$ are real symmetric and positive definite. By (iii), $D(v_E, i_I)$ is positive semidefinite. Since $J_{v,i} + J_{v,i}^t = 2\left(\begin{bmatrix} H_{EE} & 0 \\ 0 & H_{II} \end{bmatrix} + D(v_E, i_I)\right)$, $J_{v,i}$ is positive definite and is nonsingular. □

The following two cases are of particular interest.

Theorem 5. Consider a circuit characterized by (9). Assume that

(i) H is positive definite[6];

(ii) all nonlinear resistors are monotonically increasing, then the Jacobian matrix $J_{v,i}(v_E, i_I)$ defined by (19) is nonsingular for all $(v_E, i_I) \in \mathbb{R}^n$.

Proof. Since $J_{v,i} + J_{v,i}^t = (H + H^t) + 2D(v_E, i_I)$ is positive definite by (i) and (ii), $J_{v,i}$ is positive definite and nonsingular. □

Since singular points of $J_{v,i}$ and $J_\rho$ are in one-to-one correspondence if all nonlinear resistors are strictly monotonically increasing, we have

Corollary. In Theorems 4 and 5 if all nonlinear resistors are strictly monotonically increasing, then $J_\rho(\rho_E, \rho_I)$ is nonsingular for all $(\rho_E, \rho_I) \in \mathbb{R}^n$.

Remark. Observe that Theorems 4 and 5 still hold if H is positive semidefinite but all nonlinear resistors are strictly monotonically increasing.

Theorem 6. Consider a circuit characterized by (16). Assume that

(i) H is column-sum diagonally dominant, i.e., $h_{jj} > 0$, $h_{jj} \geq \sum_{\substack{i=1 \\ i \neq j}}^{n} |h_{ij}|$ for all $j \in E \cup I$;

[6] In fact, $H \in P_0$ is sufficient, see [12] and [13].

(ii) all nonlinear resistors are monotonically increasing, then the Jacobian matrix $J_\rho(\rho_E, \rho_I)$ defined by (21) is nonsingular for all $(\rho_E, \rho_I) \in \mathbb{R}^n$.

Proof. From (21), $J_\rho(\rho_E, \rho_I) = D_1(\rho_E, \rho_I) + H\, D_2(\rho_E, \rho_I)$. By assumption, $(H, D_1) \in W_0$[7] and hence $\det J_\rho(\rho_E, \rho_I) = \det (D_1 + H\, D_2) > 0$ for all $(\rho_E, \rho_I) \in \mathbb{R}^n$.

## V. THE OVERFLOW PROBLEM

In most practical cases the arc-length approach is immune to the overflow problem. It is particularly suited to diode-transistor circuits. In order to appreciate the role played by the new variable arc-length, let us consider first the conventional approach and rewrite (18) into the form

$$J_{v,i}^{(k)} \begin{bmatrix} v_E \\ i_I \end{bmatrix}^{k+1} = J_{v,i}^{(k)} \begin{bmatrix} v_E \\ i_I \end{bmatrix}^{k} - f(v_E, i_I)^k.$$

It is standard practice to solve for $(v_E, i_I)^{k+1}$ by Gaussian elimination and back substitution. Since $|di/dv|$ and $|dv/di|$ can be arbitrarily large, elements in $J_{v,i}^{(k)}$ can become extremely large and overflow problem occurs. For example, the range of non-zero real constants in the CDC 6400 computer is approximately $10^{-294}$ to $10^{+322}$, this requires the components of $v_E^k$ be less than 19 V if $v_E$ is a voltage vector across the transistor terminals. This problem can never occur if we use arc-lengths as variables. From (20),

---

[7] See [13] for a detailed discussion of properties of matrices belonging to class $W_0$.

$$J_\rho^{(k)} \begin{bmatrix} \rho_E \\ \rho_I \end{bmatrix}^{k+1} = J_\rho^{(k)} \begin{bmatrix} \rho_E \\ \rho_I \end{bmatrix}^{k} - f(\rho_E, \rho_I)^k. \qquad (23)$$

Since $\|J_\rho\|$ is bounded by a constant for all $(\rho_E, \rho_I) \in \mathbb{R}^n$ (Theorem 2), $J_\rho^{(k)}$ is well-defined for all k. There is, however, another possible source of the overflow problem. In (20), elements of $[J_\rho^{(k)}]^{-1}$ can be extremely large even though $\|J_\rho^{(k)}\|$ is bounded. This implies that overflow problem could still occur -- though much less likely -- in the process of Gaussian elimination on (23). In this section we show that under certain conditions $\|J_\rho^{-1}(\rho_E, \rho_I)\|$ is also bounded by a constant for all $(\rho_E, \rho_I) \in \mathbb{R}^n$. Obviously if this is to be the case, $J_\rho(\rho_E, \rho_I)$ must be nonsingular for all $(\rho_E, \rho_I) \in \mathbb{R}^n$. Before we present the theorems, let us consider a simple example which gives one an intuitive feeling on why the overflow problem can be overcome by choosing arc-lengths as variables.

Example.

Consider the simple transistor circuit shown in Fig. 5 (a). The network equation is given by

$$f(\rho_1, \rho_2) = \begin{bmatrix} \hat{i}_1(\rho_1) \\ \hat{i}_2(\rho_2) \end{bmatrix} + G \begin{bmatrix} \hat{v}_1(\rho_1) \\ \hat{v}_2(\rho_2) \end{bmatrix} - s \qquad (24)$$

$$= 0.$$

where

$$G \triangleq \begin{bmatrix} .1010E\text{-}2 & -.9901E\text{-}3 \\ -.1980E\text{-}6 & .1980E\text{-}4 \end{bmatrix} \quad \text{and} \quad s \triangleq \begin{bmatrix} .1198E\text{-}1 \\ -.1369E\text{-}3 \end{bmatrix}.$$

Referring to Figs. 2 (c) and (e), we observe that for $\rho < .75$, $\hat{v}(\rho) \cong \rho$ and $\hat{i}(\rho) \cong 0$. On the other hand, for $\rho > 1.25$, $\hat{i}(\rho) \cong \rho + \text{const.}$ and $\hat{v}(\rho)$ increases very slowly with $\rho$. Therefore we can divide $\mathbb{R}^2$ into regions as shown in Fig. 5 (c). On each hatched region $f(\rho_1, \rho_2)$ is approximately an affine function, i.e., a linear function plus a constant, determined by matrix G and the particular affine approximations $\hat{i}_k(\rho_k) = \rho_k + \text{const}$ and/or $\hat{v}_k(\rho_k) = \rho_k + \text{const}$. Hence, overflow problem can never occur within this region. We apply the Newton-Raphson algorithm (20) to (24). Starting at $\rho^0 = (0, 0)^t$, the iterates come close to the solution $\rho^*$ rapidly and the sequence $\{\rho^k\}$ converges to the solution with 9 digits of accuracy in 8 iterations. Notice that the initial guess $\rho^0$ is not close to the solution $\rho^* = (.63715683, -7.0436303)$ (see Fig. 5 (c)). Nevertheless, $\{\rho^k\}$ converges rapidly.

Though difficult to justify rigorously, no overflow has ever been observed even with an initial guess $\rho^0$ located in the unhatched region. In any event, observe that the area occupied by the unhatched region is much smaller compared to that occupied by the hatched region. Hence, the probability of some iterate $\rho^k$ falling within the unhatched region is indeed quite small.

We now derive rigorously some sufficient conditions which guarantee that $J_\rho^{-1}$ is bounded, thereby eliminating the only other source of the overflow problem.

Theorem 7. Consider a circuit satisfying the hypotheses of Theorem 5, i.e.,

(i) H is positive definite[8],

---

[8] In fact, $H \in P$ is sufficient. See footnote 6.

(ii) all nonlinear resistors are monotonically increasing.

Then $\|J_\rho^{-1}(\rho_E, \rho_I)\|$ exists and is bounded by a constant for all $(\rho_E, \rho_I) \in \mathbb{R}^n$.

Proof. It can be shown that[9]

$$\det J_\rho(\rho_E, \rho_I) = \sum_{j=0}^{n} [\det H\begin{pmatrix} k_1 \ldots k_j \\ k_1 \ldots k_j \end{pmatrix}] \prod_{k_i \in E} \sin\theta_{k_i} \prod_{k_i \in I} \cos\theta_{k_i} \prod_{\substack{k \in E \\ k \neq k_i}} \cos\theta_k \prod_{\substack{k \in I \\ k \neq k_i}} \sin\theta_k$$

where $1 \leq k_1 \leq k_2 \leq \ldots \leq k_j \leq n$ and $\det H\begin{pmatrix} k_1 \ldots k_j \\ k_1 \ldots k_j \end{pmatrix} \triangleq 1$ for $j = 0$.

Under the above conditions, by Appendix A5, there exists a constant $\alpha > 0$ such that

$$\det J_\rho(\rho_E, \rho_I) > \alpha \quad \text{for all } (\rho_E, \rho_I) \in \mathbb{R}^n.$$

Since $\|J_\rho(\rho_E, \rho_I)\| \leq \sqrt{\|H\|^2 + 1}$ for all $(\rho_E, \rho_I) \in \mathbb{R}^n$, by Theorem 2, we have [10]

$$\|J_\rho^{-1}(\rho_E, \rho_I)\| \leq \beta \frac{\|J_\rho(\rho_E, \rho_I)\|^{n-1}}{|\det J_\rho(\rho_E, \rho_I)|}$$

$$\leq \frac{\beta}{\alpha} (\sqrt{\|H\|^2 + 1})^{n-1} \text{ for all } (\rho_E, \rho_I) \in \mathbb{R}^n.$$

where $\beta$ and $\alpha$ are constants. □

Theorem 8. Consider a circuit characterized by (16). Assume that

(i) H is strictly column-sum diagonally dominant, i.e., $h_{jj} > 0$,

$$h_{jj} > \sum_{\substack{i=1 \\ i \neq j}}^{n} |h_{ij}| \quad \text{for all } j \in E \cup I.$$

(ii) all nonlinear resistors are monotonically increasing.

Then $J_\rho^{-1}(\rho_E, \rho_I)$ exists and is bounded by a constant for all $(\rho_E, \rho_I) \in \mathbb{R}^n$.

---

9 See Appendix A5.

Proof. By definition of the induced norm of a matrix,

$$\|J_\rho^{-1}\| \triangleq \sup_{z\neq 0} \frac{\|J_\rho^{-1} z\|}{\|z\|} \qquad z \in \mathbb{R}^n$$

$$= \sup_{z\neq 0} \frac{\|(J_\rho^{-1})^t z\|_\infty}{\|z\|_\infty} = \frac{1}{\inf\limits_{z} \frac{\|J_\rho^t z\|_\infty}{\|z\|_\infty}} = \frac{1}{\inf\limits_{\|z\|_\infty=1} \|J_\rho^t z\|_\infty} .$$

From (21),

$$J_\rho^t(\rho_E, \rho_I) = \begin{bmatrix} \cos\theta_1 + h_{11}\sin\theta_1 & h_{21}\sin\theta_1 & \cdots & h_{n1}\sin\theta_1 \\ h_{12}\sin\theta_2 & \cos\theta_2 + h_{22}\sin\theta_2 & \cdots & h_{n2}\sin\theta_2 \\ \vdots & \vdots & & \vdots \\ h_{1n}\cos\theta_n & h_{2n}\cos\theta_n & \cdots & \sin\theta_n + h_{nn}\cos\theta_n \end{bmatrix}$$

where $\cos\theta_j = d\hat{i}_j/d\rho_j$ and $\sin\theta_j = d\hat{v}_j/d\rho_j$, $j \in E \cup I$.

Without loss of generality, assume the infimum of $\|J_\rho^t z\|_\infty$ occurs at $\bar{z}$ with $|\bar{z}_k| = 1$. Now the absolute value of the k-th component of $J_\rho^t \bar{z}$ is

$$|(J_\rho^t(\rho_E, \rho_I)\bar{z})_k| = |\sin\theta_k (h_{kk} \pm \sum_{\substack{i=1 \\ i\neq k}}^{n} h_{ik}\bar{z}_i) + \cos\theta_k| \quad , k \in E$$

$$= |\cos\theta_k (h_{kk} \pm \sum_{\substack{i=1 \\ i\neq k}}^{n} h_{ik} z_i) + \sin\theta_k| \quad , k \in I. \qquad (25)$$

where the $\pm$ signs arise because $\bar{z}_k = 1$ or $-1$. By (ii), $\theta_k \in [0, \pi/2]$. By Appendix A3, the minimum of the right hand side of (25) is $\min\{h_{kk} - \sum_{\substack{i=1 \\ i\neq k}}^{n} |h_{ik}|, 1\} \triangleq \gamma$ which is positive by assumption (i). So we have

$$\inf_{\|z\|_\infty=1} \|J_\rho^t(\rho_E, \rho_I)\, z\|_\infty \geq \gamma > 0$$

Hence $\|J_\rho^{-1}(\rho_E, \rho_I)\| \leq \frac{1}{\gamma}$ for all $(\rho_E, \rho_I) \in \mathbb{R}^n$. □

Remark. It must be emphasized that the hypotheses required by Theorems 7 and 8 are only sufficient conditions which guarantee that no overflow can occur. While it is difficult to derive weaker sufficient conditions analytically, no overflow problem has ever been encountered (except when $J_\rho$ is singular) in all examples that we have so far analyzed using the arc-length approach.

## VI. CONVERGENCE PROPERTIES

We have already seen from the examples of Section I and Section V that the arc-length approach has superior convergence property over the other approaches. This is particularly significant for practical transistor and diode circuits. In all examples we have considered so far, the iterates generated by the Newton-Raphson algorithm came close to the solution rapidly even though the initial guess was chosen far away from the solution. This is highly desirable from a computational point of view because in general the success of Newton-Raphson algorithm is only guaranteed for initial guesses sufficiently close to the solution. In this section we make a comparison in the convergence property between the arc-length approach and the voltage approach[10] for transistor and diode circuits. Our analysis is based on the following theorem.

Theorem 9. ([10]) Let $f: \mathbb{R}^n \to \mathbb{R}^n$ be twice continuously differentiable. Let $z^0 \in \mathbb{R}^n$, $f(z^0) \neq 0$. Assume $J_z(z^0) = \partial f(z^0)/\partial z$ exists and is non-singular. Put $h_z^k \triangleq -J_z^{-1}(z^k)\, f(z^k)$ and $z^{k+1} = z^k + h_z^k$, $k = 0, 1, 2, \ldots$

[10] We exclude current ports just for simplicity.

as defined by the Newton-Raphson algorithm. If there exists a neighborhood $N_0$ of $z^0$ such that

(i) $\|J_z(z') - J_z(z)\| < L_z \|z' - z\|$ for all $z', z \in N_0$

i.e., $J_z$ satisfies a Lipschitz condition with a Lipschitz constant $L_z$ on $N_0$;

(ii) $[1/(L_z \|f(z^0)\| \cdot \|J_z^{-1}(z^0)\|^2)] \triangleq \zeta_z \geq 2$;

(iii) The ball $B_0 \triangleq \{z \mid \|z-z^0\| \leq r_z\}$ is contained in $N_0$, where $r_z \triangleq \{\exp[-\cosh^{-1}(\zeta_z - 1)]\} \|h_z^0\|$, then the sequence $z^k$ lies in $B_0$ and converges to the solution $z^*$ such that $f(z^*) = 0$.

Remarks. (1) It can be shown [10] that the rate of convergence depends on $\zeta_z$: the larger the $\zeta_z$, the faster the rate of convergence. Now, let $v^0$ and $\rho^0$ be the initial guesses in terms of voltages and arc-lengths, respectively, i.e., $v^0 = \hat{v}(\rho^0)$ and $f(v^0) = f(\rho^0)$. Then if $L_\rho \|J^{-1}(\rho^0)\|^2 < L_v \|J_v^{-1}(v^0)\|^2$, $\zeta_\rho > \zeta_v$ and the sequence $\{\rho^k\}$ converges faster than $\{v^k\}$.

(2) The set consisting of all $z^0$ satisfying the conditions in Theorem 9 is called a region of convergence. Suppose $\zeta_\rho > \zeta_z$. Then if $\|h_\rho^0\| \leq \|h_v^0\|$, then by (iii) $r_\rho < r_v$. That is, $\rho^1$ is closer to $\rho^*$ than $v^1$ to $v^*$. Conversely, for a fixed distance from $\rho^*$ and $v^*$, $\|v^0 - v^*\|$ must be smaller than $\|\rho^0 - \rho^*\|$ in order to have $v^1$ and $\rho^1$ within the same distance of their respective solutions. In other words, the region of convergence associated with the voltages is smaller than that associated with the arc-lengths.

(3) It is generally difficult to estimate $\|h_\rho^0\|/\|h_v^0\|$. Instead, we compare their upper bounds. Since $h_z^0 = -J_z^{-1}(z^0)f(z^0)$, an upper bound $\|\overline{h_z^0}\|$ of $\|h_z^0\|$ is $\|\overline{h_z^0}\| = \|J_z^{-1}(z^0)\| \cdot \|f(z^0)\| \leq \beta \|J_z(z^0)\|^{n-1} \cdot \|f(z^0)\| / |\det J_z(z^0)|$. It can be shown (see Theorem 10) that $\|\overline{h_v^0}\|/\|\overline{h_\rho^0}\| = (\sqrt{1+x_m^2})^{n-1} \prod_{k=1}^{n} (1/\sqrt{1+x_k^2})$, where $|x_m| = \max_k\{|x_k|\}$ and $x_k \triangleq d\hat{i}_k/dv_k$. As long as one diode is reverse-biased, i.e., $x_k \cong 0$ for some k, $\|\overline{h_\rho^0}\| < \|\overline{h_v^0}\|$.

It is generally difficult to obtain the Lipschitz constant $L_z$ for $J_z$. However, we shall use the following lemma to find an upper bound:

Lemma. ([10]) Let f be defined as in Theorem 9. The Jacobian matrix $J_z$ satisfies the Lipschitz condition

$$\|J_z(z) - J_z(z')\| \leq (\max_{\xi \in N_0} \max_k \sum_{i,j=1}^{n} \left|\frac{\partial^2 f_i(\xi)}{\partial z_k \partial z_j}\right|) \|z - z'\| \triangleq \bar{L}_z \|z - z'\|$$

for all $z, z' \in N_0$[11]. (26)

Applying (26) to (19) and (21), respectively, we obtain

$$\bar{L}_v = \max_k \left\{\left|\frac{d^2 \hat{i}_k}{dv_k^2}\right|\right\} \tag{27}$$

and

$$\bar{L}_\rho = \max_k \left\{\left|\frac{d^2 \hat{i}_k}{d\rho_k^2}\right| + h_k \left|\frac{d^2 \hat{v}_k}{d\rho_k^2}\right|\right\} \tag{28}$$

where $h_k = \sum_{j=1}^{n} |h_{kj}|$. These are fairly tight upper bounds for $L_v$ and $L_\rho$ as described in [10]. To obtain the relationship between $\bar{L}_v$ and $\bar{L}_\rho$, we substitute (13) into (28) and obtain,

$$\bar{L}_\rho = \max_k \left\{\frac{|1 + h_k x_k|}{(1 + x_k^2)^2} \left| \frac{d^2 \hat{i}_k}{dv_k^2} \right|\right\} \tag{29}$$

where $x_k \triangleq d\hat{i}_k/dv_k$, $k = 1,2, \ldots n$. We now compare the upper bounds of $L_\rho \|J_\rho^{-1}(\rho^0)\|^2$ and $L_v \|J_v^{-1}(v^0)\|^2$ for the class of transistor and diode circuits. In this case, $x_k = d\hat{i}_k/dv_k \in (0, \infty)$ and $d^2\hat{i}_k/dv_k^2 = x_k/V_T$. Moreover, for all circuits we have analyzed,[12] a conservative range of values assumed by $h_k$ is given by $h_k \sim 10^{-4}$ to $10^{-2}$. From (27) and

---

[11] We assume $N_0$ is convex.

[12] This is true for most practical circuits where the values of resistors range from a few hundred ohms to megaohms. Notice that the dimension of $h_k$ is in mhos. The symbol "~" means "of the order of".

$$(29),\ \bar{L}_\rho \le \max_k \left\{\frac{|1 + h_k x_k|}{(1 + x_k^2)}\right\} \max_k \left\{\frac{d^2\hat{i}_k}{dv_k^2}\right\} \triangleq \frac{|1 + h_\ell x_\ell|}{(1 + x_\ell^2)^2} \bar{L}_v .$$

Since $J_\rho = J_v \frac{dv}{d\rho}$, it follows from (12) that $\det J_\rho(\rho^0) = \det J_v(v^0) \prod_{k=1}^{n} [1/\sqrt{1 + x_k^2}]$. Furthermore, let $x_m \triangleq \max_k \{x_k\}$, then it follows from (19) and (21) that $\|J_v(v^0)\| \sim x_m$ and $\|J_\rho(\rho^0)\| \sim x_m/\sqrt{1 + x_m^2}$. From (27) and (29) we obtain [10]

$$L_v \|J_v^{-1}(v^0)\|^2 \le \bar{L}_v \left\{\beta \frac{\|J_v(v^0)\|^{n-1}}{|\det J_v(v^0)|}\right\}^2$$

and

$$L_\rho \|J_\rho^{-1}(\rho^0)\|^2 \le \bar{L}_\rho \left\{\beta \frac{\|J_\rho(\rho^0)\|^{n-1}}{|\det J_\rho(\rho^0)|}\right\}^2$$

where $\beta$ is a constant. Let us now define the quantity

$$\mu \triangleq \bar{L}_v \left\{\beta \frac{\|J_v(v^0)\|^{n-1}}{|\det J_v(v^0)|}\right\}^2 \Big/ \bar{L}_\rho \left\{\beta \frac{\|J_\rho(\rho^0)\|^{n-1}}{|\det J_\rho(\rho^0)|}\right\}^2 ,$$

henceforth called the convergence-region-enlargement ratio because it provides a quantitative measure of the enlargement of the region of convergence associated with the arc-length approach over that associated with the voltage approach. Observe that the higher the value of $\mu$, the larger is the region of convergence of the arc-length approach as compared to that of the voltage approach. For ease of comparison, the following theorem provides a useful estimate for $\mu$:

Theorem 10. The convergence-region-enlargement ratio $\mu$ can be estimated by

$$\mu \sim \frac{1 + x_\ell^2}{|1 + h_\ell x_\ell|} \prod_{\substack{k=1 \\ k \neq \ell}}^{n} \left\{\frac{1 + x_m^2}{1 + x_k^2}\right\} .$$

Proof.

$$\bar{L}_\rho \left\{ \beta \frac{\|J_\rho(\rho^0)\|^{n-1}}{|\det J_\rho(\rho^0)|} \right\}^2 \leq \bar{L}_v \frac{|1 + h_\ell x_\ell|}{(1 + x_\ell^2)} \left\{ \beta \frac{\|J_\rho(\rho^0)\|^{n-1}}{|\det J_\rho(\rho^0)|} \right\}^2$$

$$\sim \bar{L}_v \frac{|1 + h_\ell x_\ell|}{(1 + x_\ell^2)} \left\{ \beta \frac{\|J_v(v^0)\|^{n-1} (1/\sqrt{1 + x_m^2})^{n-1}}{|\det J_v(v^0)| \prod_{k=1}^{n} (1/\sqrt{1 + x_k^2})} \right\}^2$$

$$= \bar{L}_v \left\{ \beta \frac{\|J_v(v^0)\|^{n-1}}{|\det J_v(v^0)|} \right\}^2 \frac{|1 + h_\ell x_\ell|}{(1 + x_\ell^2)} \prod_{\substack{k=1 \\ k \neq \ell}}^{n} \left\{ \frac{1 + x_k^2}{1 + x_m^2} \right\}$$

where the denominator $(1 + x_m^2)$ is understood to be repeated $(n - 1)$ times when evaluating the terms associated with the product operation $\Pi$. Comparing the last term with the first term we obtain the estimate for $\mu$. □

For practical circuits, $h_\ell \sim 10^{-4}$ to $10^{-2}$, minimizing $(1 + x_\ell^2)/|1 + h_\ell x_\ell|$ with respect to $x_\ell$, we obtain $\min_{x_\ell} [(1 + x_\ell^2)/|1 + h_\ell x_\ell|] \cong 1/(1 + \frac{1}{4} h_\ell^2) \sim 1$. This means that $\mu \sim \prod_{\substack{k=1 \\ k \neq \ell}}^{n} [(1 + x_m^2) / (1 + x_k^2)]$.

An inspection of Fig. 2 (b) shows that in a neighborhood of $v^0$ or $\rho^0$ containing the solution, $x_m$ changes from $10^{-2}$ to $10^3$ corresponding to $v_m$ changing from .5v to .85v. Taking $x_m = 10$ for example, we find from above that $\mu \sim 10^{2N}$ where N is the number of diodes which are reverse biased ($x_k \cong 0$ if the k-th diode is reverse biased). The fact that $\mu$ increases exponentially with N is very significant. The more transistors and diodes the circuit contains, the higher the $\mu$ and the more advantageous the arc-length approach over the voltage approach. We will now supplement the preceding analytical arguments with some geometrical interpretations with the help of the following examples.

Example 1. Consider the same circuit in Fig. 1 (a) with E = 1 v and R = 1 K. We plot the functions f(v) and f(ρ) in Fig. 6 using two sets of vertical scales. Notice that for large values of v and ρ (see Figs. 6 (c) and (d)), f(v) is exponential while f(ρ) is almost a straight line. It follows that the iteration must converge much more rapidly in the latter case.

Example 2. Consider the simple transistor circuit shown in Fig. 5 (a). We try four different initial guesses and plot the corresponding loci of the Newton-Raphson iterates in the $v_1 - v_2$ plane in Fig. 7 (a) and in the $\rho_1 - \rho_2$ plane in Fig. 7 (b). In both cases, the dotted lines pertain to the conventional voltage-variable approach while the solid lines pertain to the arc-length approach. For comparison purposes the loci in Fig. 7 (a) corresponding to the arc-length $\rho_1$ and $\rho_2$ are expressed in terms of voltages $v_1(\rho_1)$ and $v_2(\rho_2)$. Similarly, in Fig. 7 (b), the loci corresponding to voltages $v_1$ and $v_2$ are expressed in terms of arc-lengths $\rho_1(v_1)$ and $\rho_2(v_2)$. In the figure, heavy bold lines mean a group of points. An inspection of Fig. 7 (a) shows that the respective loci for the initial guess "I" converge to the solution in 15 iterations using the arc-length approach, and 102 iterations using the conventional approach. The conventional approach terminates prematurely due to overflow when the initial guess is chosen at points II, III and IV. On the other hand, the arc-length approach converges in 15, 8 and 10 iterations respectively. The preceding observations are summarized in Table 2.

Table 2. Comparison of the convergence behavior in terms of voltages and arc-lengths for 4 different initial guesses.

| Initial Guess | | | Iteration on Voltage | Iteration on Arc-length |
|---|---|---|---|---|
| Point | $v^0$ | $\rho^0 = \rho(v^0)$ | | |
| I | (3,3) | (1.3E37,1.3E37) | 102 | 15 |
| II | (-3,3) | (-3,1.3E37) | overflow after 58 iterations | 15 |
| III | (-3,-3) | (-3,-3) | overflow after 1 iteration | 8 |
| IV | (3,-3) | (1.3E37,-3) | overflow after 2 iterations | 10 |

The superior convergence property of the arc-length iteration exhibited in Table 2 can be explained intuitively upon noting that the Lipschitz constant $\bar{L}_\rho$ of $J_\rho$ associated with the initial guess is extremely small (since $x_m$ is either very large or very small) and the function $f(\rho)$ defined by (24) behaves like an affine function. Since the Newton-Raphson algorithm converges in one step for affine functions, the sequence $\{\rho^k\}$ approaches the solution $\rho^*$ rapidly. Finally, we remark that since the diode voltage in the Ebers-Moll transistor model in most practical transistor circuits seldom exceeds 0.7 volt, it is reasonable to always choose the origin ($\rho_k^0 = 0$) as the initial guess when H is nonsingular and the point $\rho_k^0 = 0.6$ for all k when H is singular. In these cases, we are sure that both the initial guess $\rho^0$ and the solution $\rho^*$ will lie in the same connected region where $f(\rho)$ may be represented by an affine approximation. (See Fig. 5 (c)).

## VII. EXAMPLES

We will illustrate the arc-length approach by a few examples. Whenever possible, the network equations will be solved by the Newton-

Raphson method. When the Jacobian matrix becomes singular, we switch to the steepest descent method with Golden section search for appropriate step sizes. For comparison, we always start from the same initial guess $\rho^0 = 0 \in \mathbb{R}^n$. All examples show rapid convergence and no overflow. We have also tried to solve the same problems using the conventional voltage and current approaches but all iterations were terminated prematurely due to overflow. In the following examples, the precision is 8 digits after the decimal point.

Example 1. Consider the circuit shown in Fig. 8 (a). The network equation is given by

$$\hat{i}_E(\rho_E) + H_{EE}\hat{v}_E(\rho_E) - s = 0$$

where

$$H = \begin{bmatrix} .1313E\text{-}3 & -.1005E\text{-}3 & .1005E\text{-}3 & -.9272E\text{-}4 \\ .1512E\text{-}4 & .2872E\text{-}4 & -.2872E\text{-}4 & .2650E\text{-}4 \\ .1225E\text{-}3 & -.1367E\text{-}3 & .1367E\text{-}3 & -.1049E\text{-}3 \\ .1529E\text{-}4 & -.1707E\text{-}4 & .1707E\text{-}4 & .2674E\text{-}4 \end{bmatrix}$$

and $s = [-.2704E\text{-}2 \quad .1410E\text{-}3 \quad -.2792E\text{-}2 \quad .4958E\text{-}4]^t$.

Solution. $v_1 = .61792024$ v. $\quad v_2 = -.13904286E1$ v.

$v_3 = .61765611$ v. $\quad v_4 = -.34968589E1$ v.

Number of iterations: 8.

Example 2. Consider the voltage inverter shown in Fig. 8 (b). The circuit is characterized by the same equation as that in Example 1 with

$$H = \begin{bmatrix} .3369E-2 & -.2403E-2 & -.4713E-2 & .0 & .0 & .0 \\ .9082E-3 & .4807E-4 & .9425E-5 & .0 & .0 & .0 \\ -.9425E-3 & .9425E-3 & .3365E-2 & -.2403E-2 & -.4713E-3 & .0 \\ -.9331E-3 & .9331E-3 & .9037E-3 & .4807E-4 & .9425E-5 & .0 \\ .0 & .0 & -.9425E-3 & .9425E-3 & .2903E-2 & -.1941E-2 \\ .0 & .0 & -.9331E-3 & .9331E-3 & .9129E-3 & .3883E-4 \end{bmatrix}$$

and

$$s = [-.1642E-1 \quad -.4550E-2 \quad -.1171E-1 \quad .1199E-3 \quad -.1176E-1 \quad .1210E-3]^t$$

Solution. $v_1 = .67036572$ v. $v_2 = .63411683$ v.
$v_3 = .15323978$ v. $v_4 = -.48025058E1$ v.
$v_5 = .67039247$ v. $v_6 = .63383432$ v.

Number of iterations: 9.

Example 3. Consider the operational amplifier circuit shown in Fig. 8 (c).

This circuit is characterized by

$$\begin{bmatrix} \hat{i}_k(\rho_1) \\ \vdots \\ \hat{i}_{19}(\rho_{19}) \\ \hat{v}_{20}(\rho_{20}) \\ \vdots \\ \hat{v}_{22}(\rho_{22}) \end{bmatrix} + H \begin{bmatrix} \hat{v}_1(\rho_1) \\ \vdots \\ \hat{v}_{19}(\rho_{19}) \\ \hat{i}_{20}(\rho_{20}) \\ \vdots \\ \hat{i}_{22}(\rho_{22}) \end{bmatrix} - s = 0.$$

where H is a 22 x 22 matrix. Entries of H and s are listed in Appendix A6.

Solution. $v_1 = .62426857$ v. $v_2 = -.34935916E1$ v.
$v_3 = .61721934$ v. $v_4 = -.15696097E1$ v.
$v_5 = .62985911$ v. $v_6 = -.86511997$ v.
$v_7 = .63475472$ v. $v_8 = -.36300723E1$ v.
$v_9 = .63409094$ v. $v_{10} = .64239200$ v.

$v_{11}$ = -.34219597E1 v. $v_{12}$ = .64239475 v.

$v_{13}$ = -.86217929 v $v_{14}$ = .63500900 v.

$v_{15}$ = .63500900 v. $v_{16}$ = .60293795 v.

$v_{17}$ = -.20786375E-3v. $v_{18}$ = .62404612 v.

$v_{19}$ = -.16910235E1 v. $v_{20}$ = -.29392223E1 v.

$v_{21}$ = -.94820172E1 v. $v_{22}$ = -.10174531E2 v.

Number of iterations: 25.

## VIII. CONCLUDING REMARKS

In this paper we have presented a new approach which overcomes the slow convergence and overflow problems commonly encountered in the computer analysis of circuits containing nonlinear resistors characterized by rapidly varying nonlinearities. Theoretically speaking, since arc-lengths can be used to describe resistors which are neither voltage nor current controlled, our approach is also more general than nodal analysis. Computationally, since the convergence properties can be improved greatly by appropriate assignment of voltage and/or current ports, our approach is generally superior to other methods. For practical diode-transistor circuits, the improvement in the rate of convergence of the arc-length approach over the conventional approach increases remarkably as the size of the circuit increases. Therefore the arc-length approach is particularly suited for analyzing practical large-scale electronic circuits. Finally, in this connection we would like to point out that even though the hybrid matrix is generally not as sparse as the nodal admittance matrix, it is usually of a much lower dimension and in many cases the hybrid matrix can be made sparse

by introducing "dummy ports". For example, consider the same circuit in Example 1 of Section VI. Introducing one more voltage port by connecting a linear resistor with a very high resistance across nodes a and b as shown in Fig. 9, the hybrid matrix H becomes

$$H = \begin{bmatrix} .1980E-3 & -.1750E-3 & 0. & 0. & -.1750E-3 \\ -.3960E-5 & .5001E-4 & 0. & 0. & .5001E-4 \\ 0. & 0. & .3211E-3 & -.2750E-3 & .3211E-3 \\ 0. & 0. & .4009E-4 & .5501E-5 & .4009E-4 \\ -.2000E-3 & .2233E-3 & .3010E-3 & -.2778E-3 & .5243E-3 \end{bmatrix}$$

which contains two blocks of zeros since port 5 cuts the circuit into two separate ports. Even though the saving in computation is not particularly remarkable for this simple circuit, it can become very significant for large circuits.

ACKNOWLEDGEMENT

The authors would like to thank Dr. T. Roska for his careful reading of an earlier version of this paper and for offering several suggestions.

## APPENDIX

### A1. Diode Characteristic as a Function of Arc-length

It follows from the diode characteristic $\hat{i}(v) = I_s(e^{v/V_T} - 1)$ that $d\hat{i}/dv = \theta e^{v/V_T} \triangleq x$, where $\theta \triangleq I_s/V_T$. Choosing (0,0) as the starting point of the arc-length $\rho$, we have

$$\rho(v) = \int_0^v \sqrt{1 + \left(\frac{d\hat{i}}{dv'}\right)^2}\, dv' = \int_0^v \sqrt{1 + x^2}\, dv$$

$$= -V_T \int_{\tan^{-1}\theta}^{\tan^{-1}x} \left\{\frac{1}{\sin\psi \cos^2\psi}\right\} d\psi, \text{ where } \tan\psi = x$$

$$= V_T \left\{\frac{1}{\cos\psi} + \log\tan\frac{\psi}{2}\right\}_{\psi=\tan^{-1}\theta}^{\tan^{-1}x} = V_T\left\{\log\left(\frac{x}{1+\sqrt{1+x^2}}\right) + \sqrt{1+x^2}\right\} + c_1$$

where $c_1 = -V_T\left\{\log\left(\frac{\theta}{1+\sqrt{1+\theta^2}}\right) + \sqrt{1+\theta^2}\right\}$.

### A2. Temperature Modification

Instead of solving for v and i as functions of $\rho$, we find relations between the normalized variables $v/V_T$, $i/V_T$ and $\rho/V_T$. From (14) and (15)

$$v/V_T = \log x - \log\theta \quad \text{and} \quad i/V_T = x - \theta \tag{30}$$

and

$$\rho/V_T = \sqrt{1+x^2} + \log\left(\frac{x}{1+\sqrt{1+x^2}}\right) + c_2 \tag{31}$$

where

$$c_2 \triangleq \frac{c_1}{V_T} = -\sqrt{1+\theta^2} - \log\left(\frac{\theta}{1+\sqrt{1+\theta^2}}\right). \tag{32}$$

Choosing $T_0 = 298°$ K so that $V_{T_0} \cong 0.026$ v, we compute $v/V_{T_0}$ and $i/V_{T_0}$ as functions of $\rho/V_{T_0}$ and have them tabulated. Given $\rho$, it is easy to find $v(\rho)$ and $i(\rho)$ from the table. Notice that $v/V_{T_0}$, $i/V_{T_0}$

and $\rho/V_{T_0}$ depend only on x and the constants $c_2$ and $\theta$ at $T_0$. Call these functions (of x) $\hat{v}/V_{T_0}$, $\hat{i}/V_{T_0}$, and $\hat{\rho}/V_{T_0}$ respectively. In case the temperature $T \neq T_0$, it follows from $I_s = I_{s_0}\, e^{0.08(T-T_0)}$ and $V_T = kT/q$ that $\theta = I_s/V_T = \theta_0(T_0/T)e^{0.08(T-T_0)}$ where the subscript 0 designates quantities associated with $T_0$. Since $\theta << 1$, it follows from (32) that[13]

$$c_2 \cong -1 - \log(\frac{\theta}{2}) = -(1 + \log 2) - \log[\theta_0(\frac{T_0}{T})e^{0.08(T-T_0)}]$$

$$= c_{20} + [\log(\frac{T}{T_0}) - 0.08(T - T_0)]$$

where $c_{20} = -1 - \log(\frac{\theta_0}{2})$. If we subtract equations (30), (31) and (32) at temperature $T_0$ from the corresponding expressions at temperature T, we would obtain

$$\rho/V_T = \hat{\rho}/V_T + (c_2 - c_{20}) = \hat{\rho}/V_T + [\log(\frac{T}{T_0}) - 0.08(T-T_0)]$$

$$v/V_T = \hat{v}/V_T - \log(\frac{\theta}{\theta_0}) = \hat{v}/V_T - 0.08(T - T_0)$$

and $i/V_T = \hat{i}/V_T - (\theta - \theta_0)$.

The following algorithm can now be given for computing the diode voltage and current at any temperature T:

Step 0. Given $T \neq T_0$, compute $V_T$, $I_s$ and $\theta$.

Step 1. Given $\rho$, compute the normalized arc-length

$$\rho_N \triangleq \hat{\rho}/V_{T_0} = \rho/V_T + 0.08(T - T_0) - \log(T/T_0).$$

Step 2. Look up the table, find $(v/V_{T_0})(\rho_N)$ and $(i/V_{T_0})(\rho_N)$.

Step 3. Compute

$$v(\rho) = V_T[(v/V_{T_0})(\rho_N) - \log(\theta/\theta_0)] \text{ and}$$

$$i(\rho) = V_T[(i/V_{T_0})(\rho_N) - (\theta - \theta_0)].$$

---

[13] $\theta \leq 10^{-7}$ for $|T - T_0| \leq 125°$ K.

Remarks. (1) The above procedure is based on the assumption that

$|T - T_0| \leq 125°$ K.

(2) Constants in the formulas should be precalculated once T is fixed.

A3. A Lemma

Let $f(\theta) = a \cos \theta + b \sin \theta$; $a \geq 0$, $b \geq 0$ and $\theta \in [0, \pi/2]$, then $\max f = \sqrt{a^2 + b^2}$ and $\min f = \min \{a, b\}$.

Proof. $\frac{df}{d\theta} = - a \sin \theta + b \cos \theta = 0$.

Solving for $\theta$, we obtain

$$\theta = \theta_M \triangleq \tan^{-1}(\frac{b}{a}) \text{ and } f(\theta_M) = \sqrt{a^2 + b^2}.$$

The value $\theta_M$ gives obviously the unique maximum. The minimum occurs at $\theta = 0$ or $\theta = \pi/2$.

A4. The Determinant of $J_\rho(\rho_E, \rho_I)$

The expression for $\det J_\rho (\rho_E, \rho_I)$ can be obtained by successive expansions along columns of $J_\rho(\rho_E, \rho_I)$. The proof follows from direct computation and induction. For example, consider the simple case

$$\det J_\rho(\rho_1, \rho_2) = \begin{vmatrix} \cos \theta_1 + h_{11} \sin \theta_1 & h_{12} \cos \theta_2 \\ h_{21} \sin \theta_1 & \sin \theta_2 + h_{22} \cos \theta_2 \end{vmatrix}$$

$$= \cos \theta_1 ( \sin \theta_2 + h_{22} \cos \theta_2) + \sin \theta_1 \begin{vmatrix} h_{11} & h_{12} \cos \theta_2 \\ h_{21} & \sin \theta_2 + h_{22} \cos \theta_2 \end{vmatrix}$$

$$= \cos \theta_1 (\sin \theta_2 + h_{22} \cos \theta_2) + (\sin \theta_1)[h_{11} \sin \theta_2 + \begin{vmatrix} h_{11} & h_{12} \\ h_{21} & h_{22} \end{vmatrix} \cos \theta_2]$$

$$= \cos\theta_1 \sin\theta_2 + h_{11} \sin\theta_1 \sin\theta_2 + h_{22} \cos\theta_1 \cos\theta_2 +$$

$$(\det H) \sin\theta_1 \cos\theta_2.$$

A5. Minimum of $\det J_\rho(\rho_E, \rho_I)$

We claim that $\det J_\rho(\rho_E, \rho_I) > \alpha$ for some $\alpha > 0$. The proof is straightforward but lengthy. Here we just use the simple case from A4 to illustrate the point.

$$\det J_\rho(\rho_1, \rho_2) = [(\det H) \cos\theta_2 + h_{11} \sin\theta_2] \sin\theta_1 +$$

$$[h_{22} \cos\theta_2 + \sin\theta_2] \cos\theta_1$$

Notice that $\theta_j \in [0, \pi/2]$. Minimizing the right hand side over $\theta_1$, we obtain the following expression with the help of A3:

$$\min_{\theta_1} \det J_\rho(\rho_1, \rho_2) = \min\{[(\det H) \cos\theta_2 + h_{11} \sin\theta_2],$$

$$[h_{22} \cos\theta_2 + \sin\theta_2]\}.$$

Minimizing over $\theta_2$ again we obtain

$$\min_{\theta_1,\theta_2} \det J_\rho(\rho_1, \rho_2) = \min\{\det H, h_{11}, h_{22}, 1\} \triangleq \alpha > 0$$

since H is positive definite. The case of higher dimensions follows by induction.

## REFERENCES


[1] Davidenko, D.F., "On a new method of numerical solution of systems of nonlinear equations", Dokl. Akad., Nauk SSSR, vol. 88, 1953, pp. 601-602.

[2] Polak, E., Computational Methods in Optimization. Academic Press, 1971.

[3] Armijo, L., "Minimization of functions having continuous partial derivatives", Pacific J. Math., 16, 1966, pp. 1-3.

[4] Nagel, L. and R.A. Rohrer, "Computer analysis of nonlinear circuits, excluding radiation (CANCER)", IEEE J. of Solid State Circuits, Vol. SC-6, Aug. 1971, pp. 166-182.

[5] Calahan, D.A., Computer-Aided Network Design. McGraw-Hill, Inc., 1972.

[6] Lin, P.M., "Formulation of hybrid matrices for linear multiports containing controlled sources", IEEE Trans. on Circuits and Systems, vol. CAS-21, No. 2, March 1974, pp. 169-175.

[7] Chung, S.H. and P.H. Roe, "Formulation and properties of hybrid matrices for (m + n)-port R networks", IEEE Trans. on Circuit Theory, May 1970, pp. 243-245.

[8] Chua, L.O. and R.A. Rohrer, "On the dynamic equations of a class of nonlinear RLC networks", IEEE Trans. on Circuit Theory, Dec. 1965, pp. 475-489.

[9] So, H.C., "On the hybrid description of a linear n-port resulting from extraction of arbitrarily specified elements", IEEE Trans. Circuit Theory, vol. CT-12, Sept. 1965, pp. 381-387.

[10] Ostrowski, A.M., Solution of Equations in Euclidean and Banach Spaces. Academic Press, 1973.

[11] Apostol, T.N., Mathematical Analysis, A Modern Approach to Advanced Calculus, Addison-Wesley, Reading, MA, 1957.

[12] Fiedler, M. and Ptak, V., "Some generalizations of postive definiteness and monotonicity", Numer. Math. 9, pp. 163-172 (1966).

[13] Willson, A.N. Jr., "New theorems on the equations of nonlinear dc transistor networks", Ibid., 49 (1970), pp. 1713-1738.

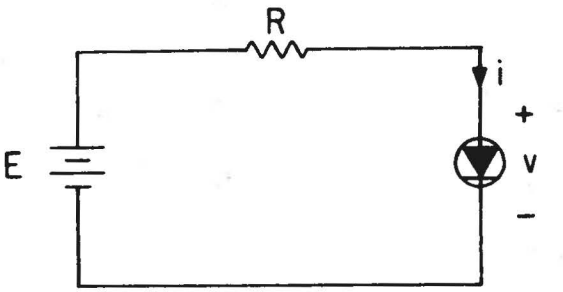


(a)

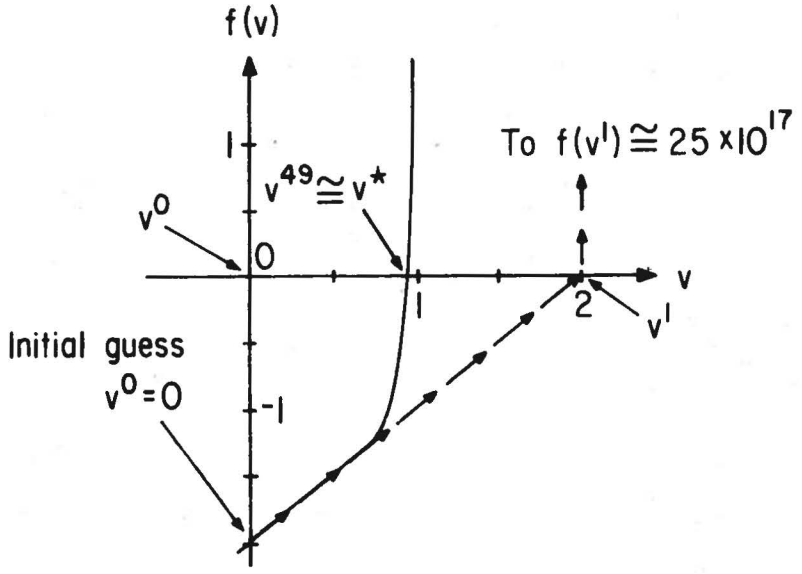


(b)

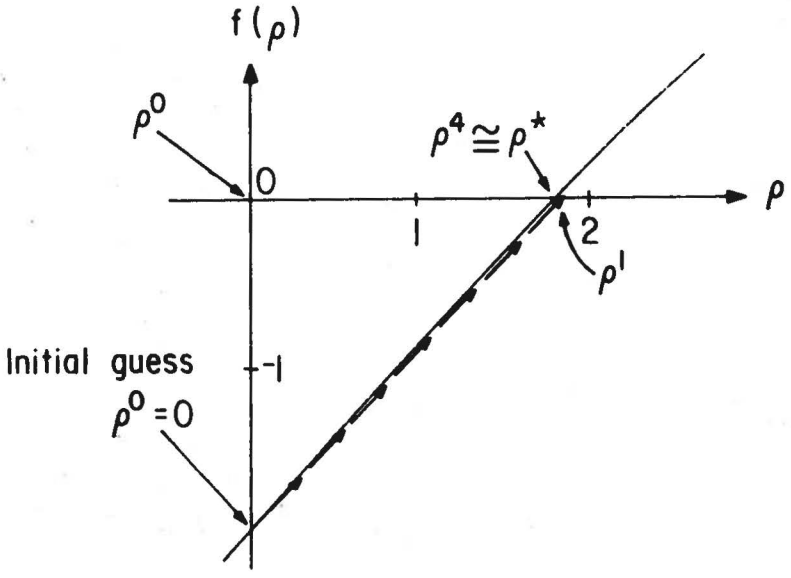


(c)

Fig. 1. A simple diode circuit. (a) The circuit diagram; (b) The function f(v) defined by Eq. (2) corresponding to E = 2v and R = 1 ohm. Starting at $v^\circ = 0$, the sequence $\{v^k\}$ generated by Newton-Raphson iteration converges very slowly; after 49 iterations. (c) The function f(ρ) defined by (4) corresponding to E = 2v and R = 1 ohm. Starting at $\rho^\circ = 0$, the sequence $\{\rho^k\}$ generated by Newton-Raphson iteration converges extremely rapidly, after 4 iterations.

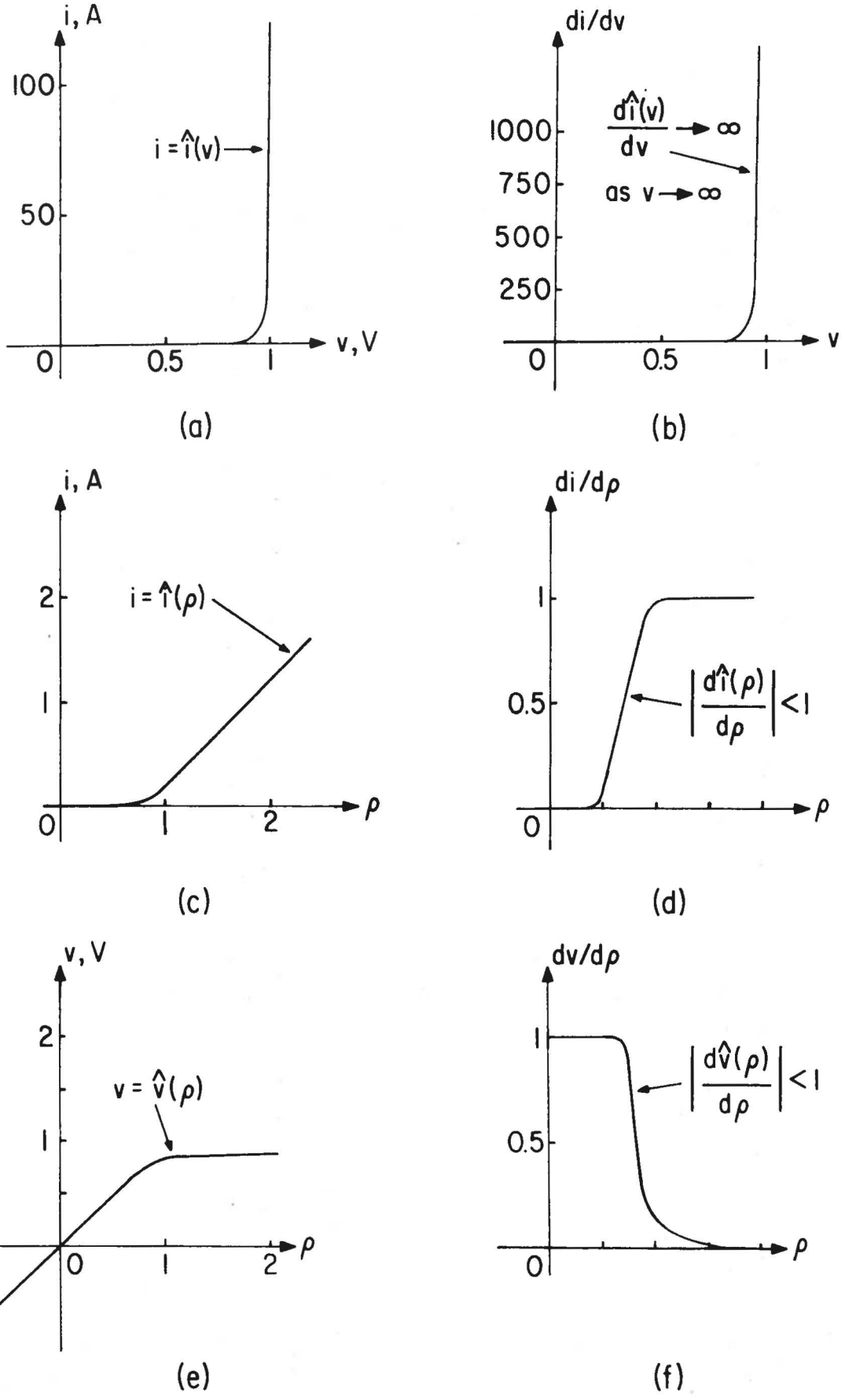


**Fig. 2** Characteristics of a diode with $I_s = 10^{-13}$ A and $V_T = .026$ V.

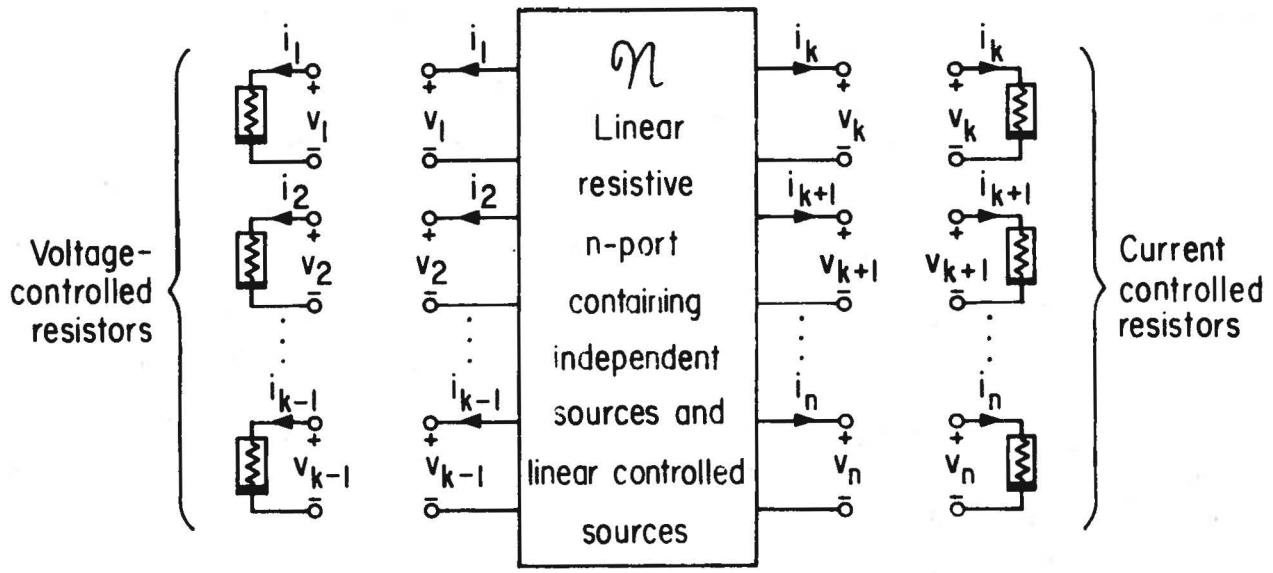


Fig. 3. Linear resistive n-parts terminated by nonlinear resistors, diodes and transistors. (a) The ports are terminated by nonlinear resistors. (b) The transistors are replaced by diode-controlled source combinations so that $\mathcal{N}'$ does not contain any controlled sources.

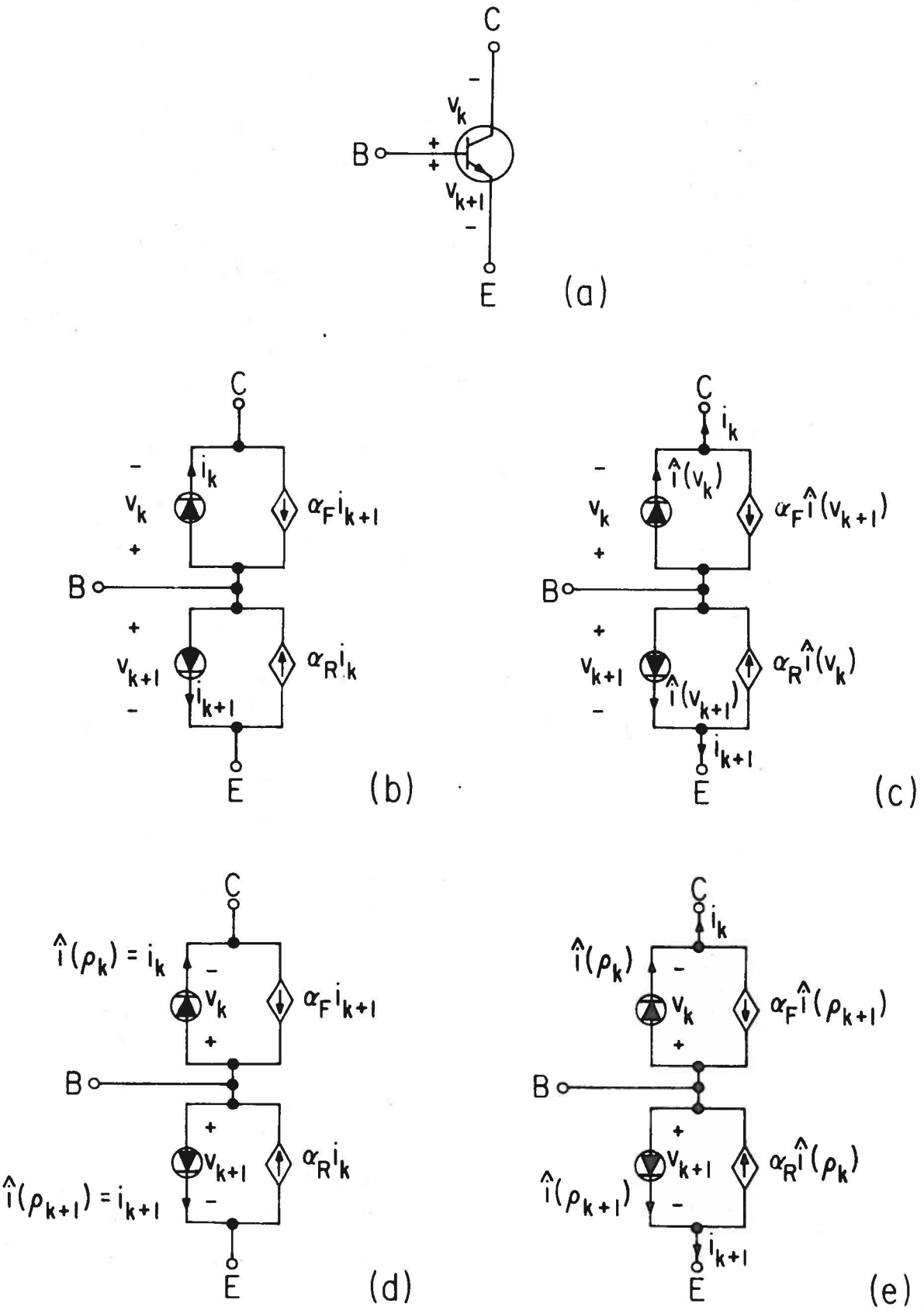


Fig. 4. The Ebers-Moll model of an npn bipolar junction transistor in various equivalent forms.

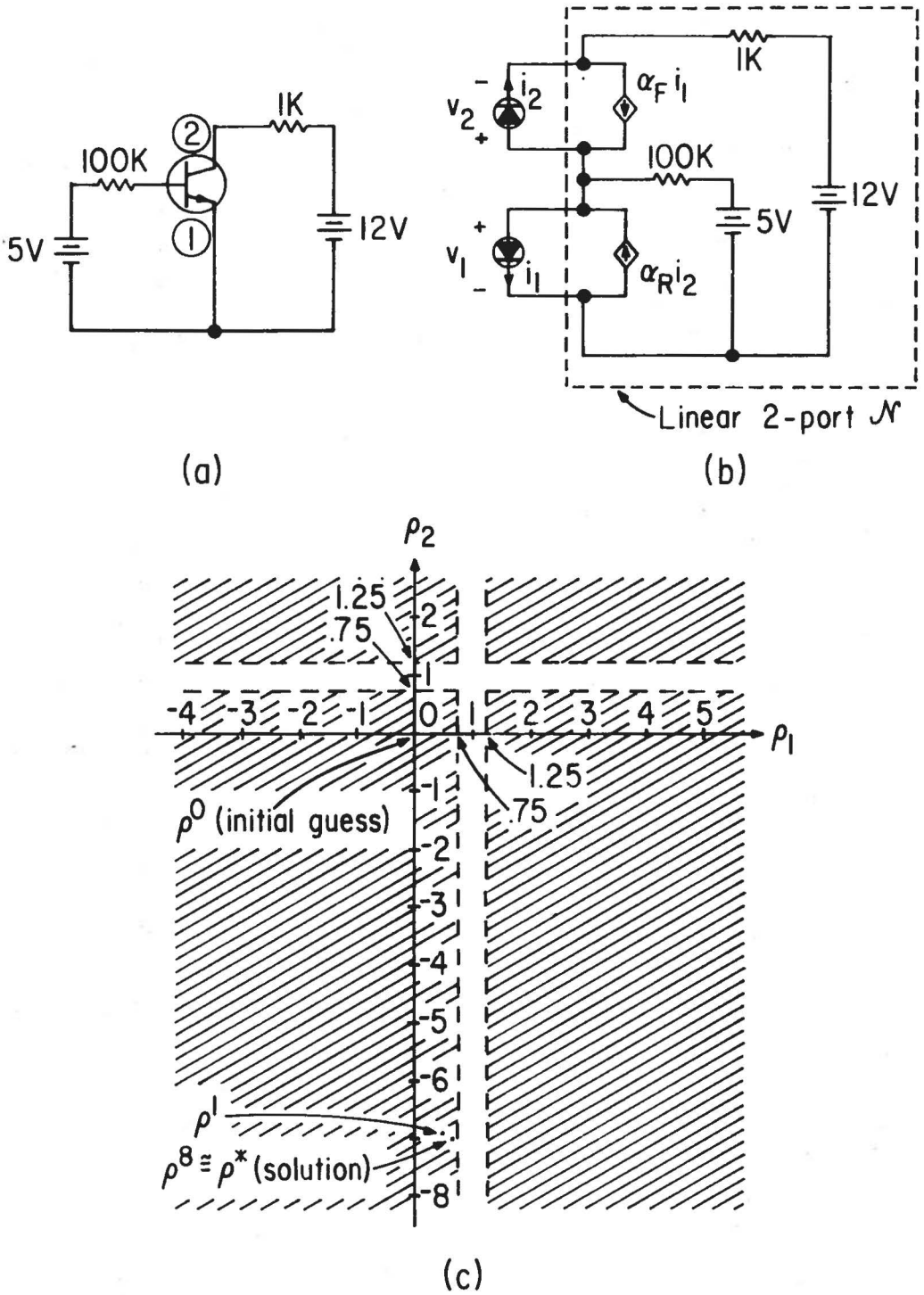


Fig. 5. A simple transistor circuit. (a) The circuit diagram; (b) The 2-port obtained by extracting the nonlinear resistors (the diodes) as voltage ports. Notice that the port voltage and current are related by associated reference directions; (c) Regions of affine approximations of $f(\rho)$. In each hatched region $f(\rho)$ behaves like an affine function of $\rho$.

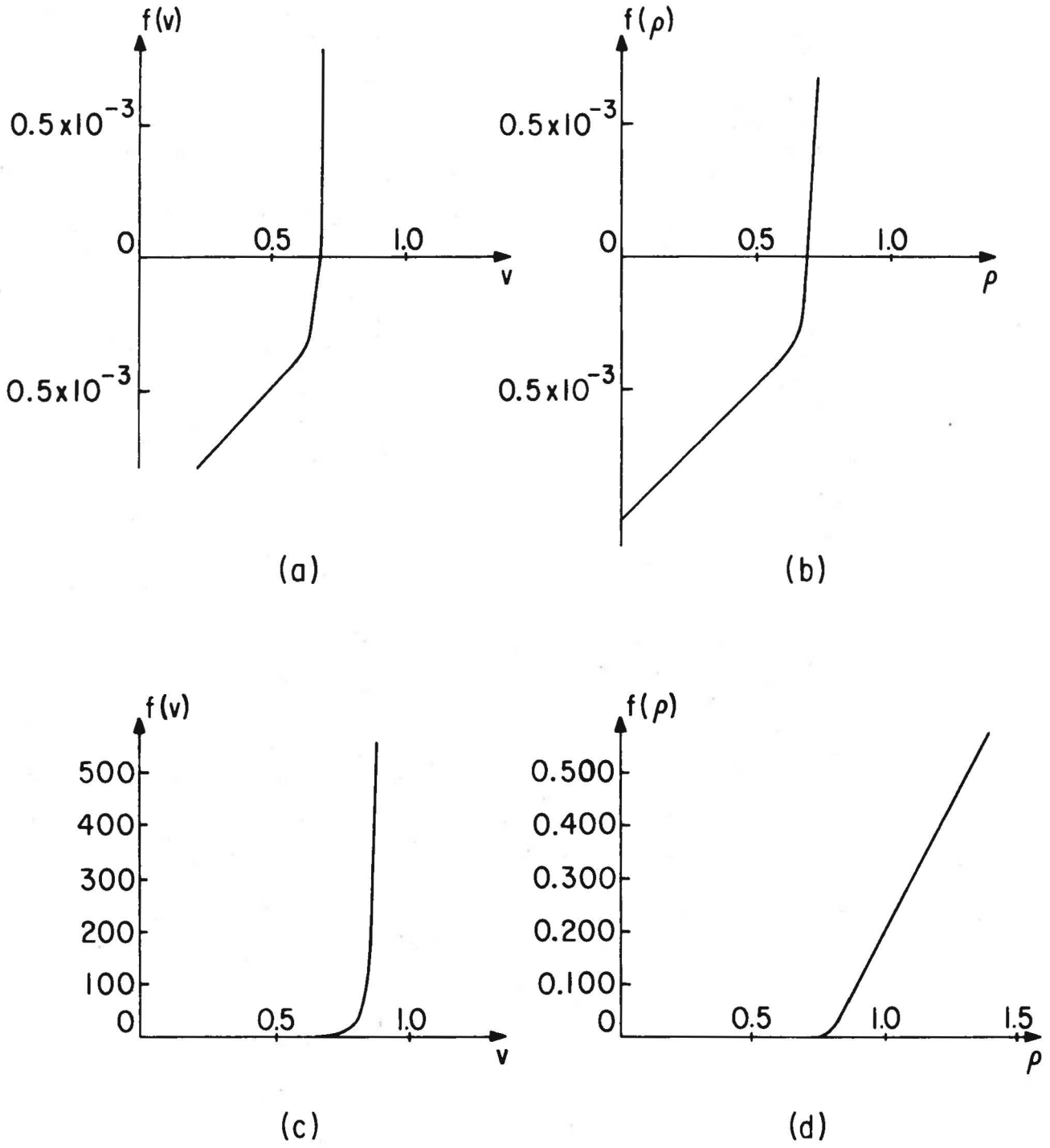


Fig. 6. Functions f(v) and f(ρ) for the simple diode circuit shown in Fig. 1 (a) corresponding to E = 1 v and R = 1 K ohm. (a) and (b) For small values of v and ρ, f(v) and f(ρ) resemble each other. (c) and (d) For large values of v and ρ, f(v) is exponential while f(ρ) is almost a straight line.

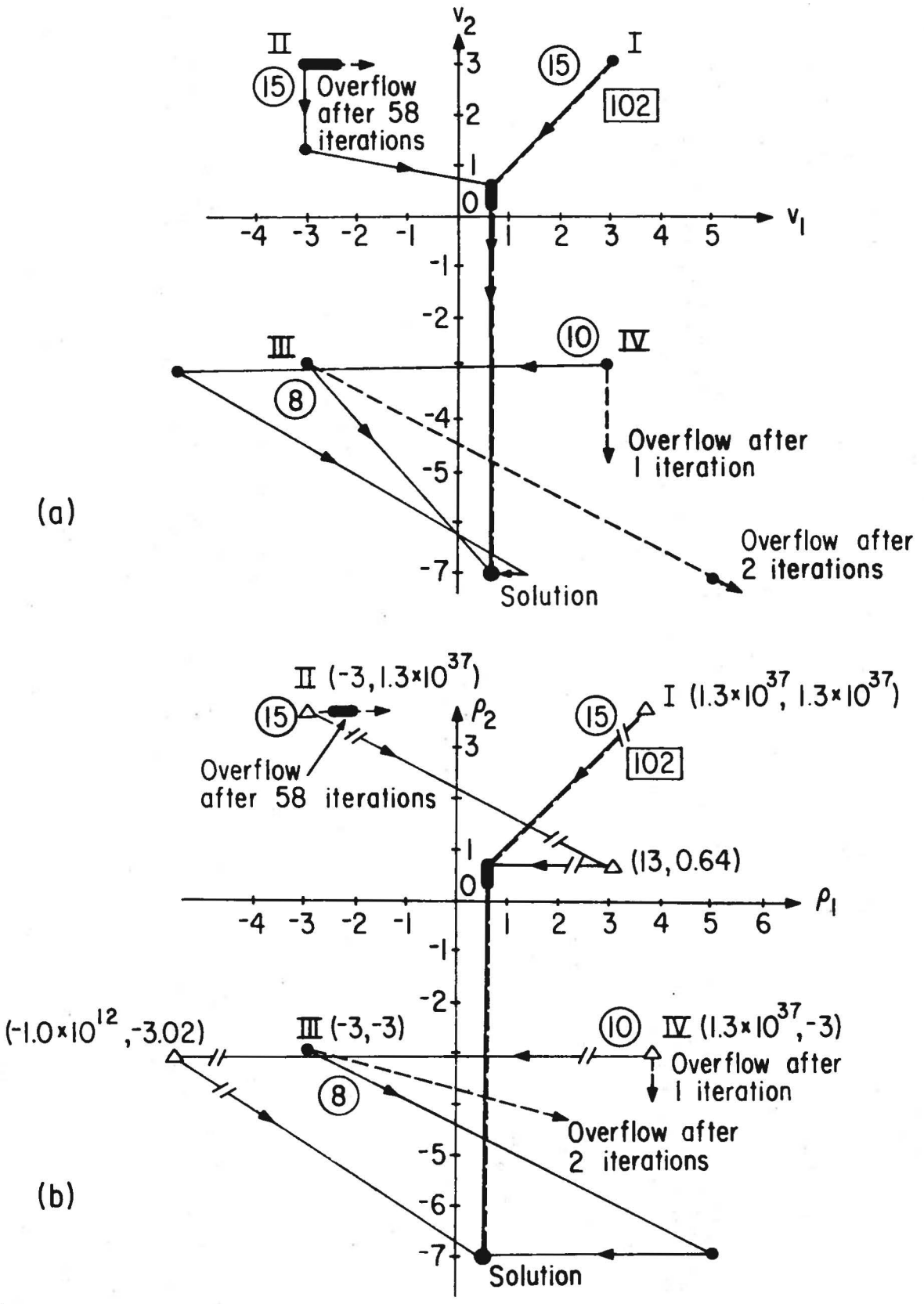


Fig. 7. Comparison of Newton-Raphson iterations between the voltage approach and the arc-length approach. The heavy bold segments indicate a group of points clustered near each other. Solid lines denote loci of iterates $\hat{v}(\rho^k)$ in (a) and $\rho^k$ in (b). Dotted lines denote loci of iterates $v^k$ in (a) and $\rho(v^k)$ in (b). Single dots in the graph denote actual position of a point while "triangles" $\Delta$ denote remote points lying outside of the normal scale indicated.

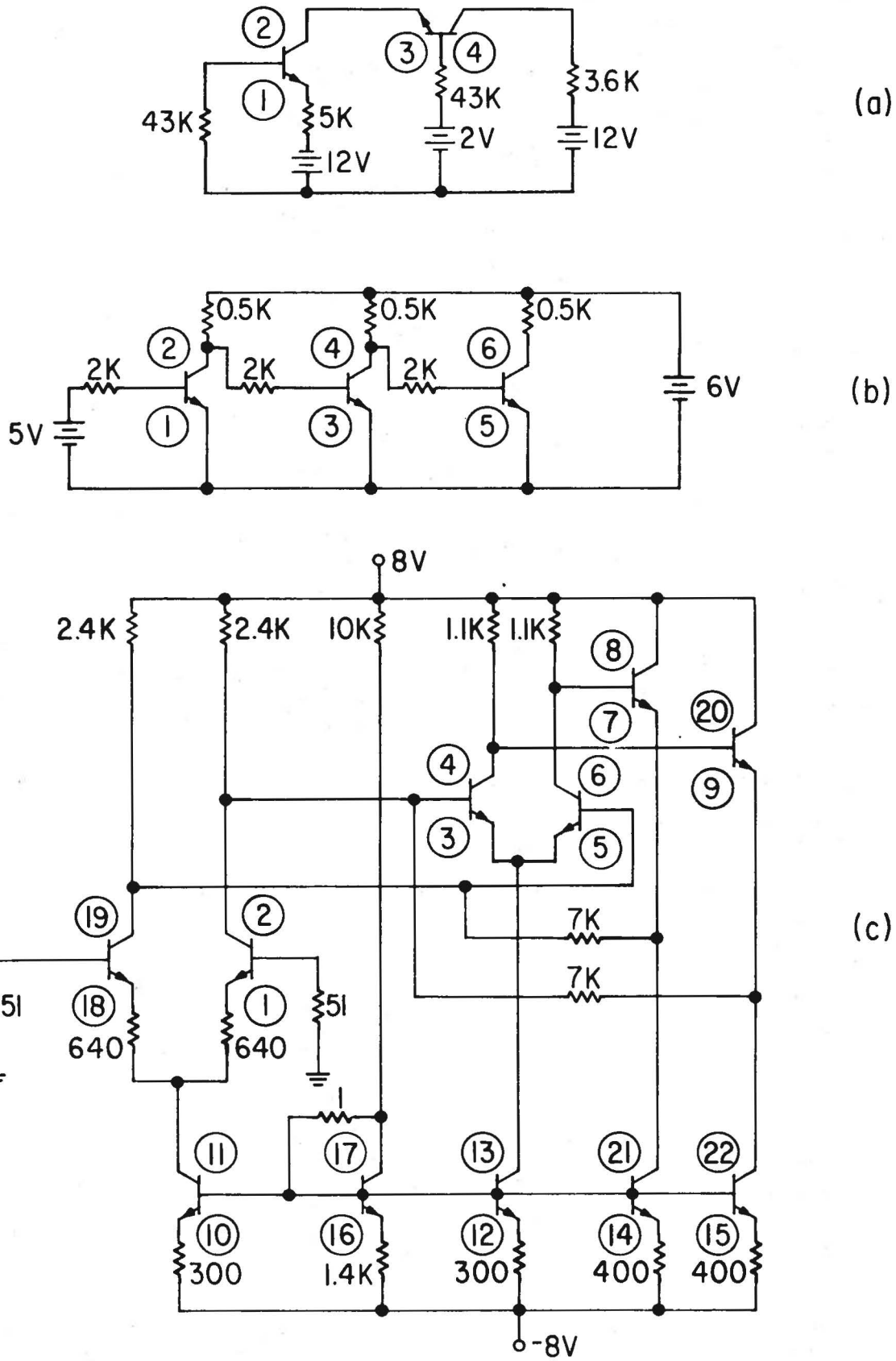


Fig. 8. Transistor circuits for the example in Section VII. (a) Circuit for example 1; (b) Circuit for example 2; (c) Circuit for example 3.

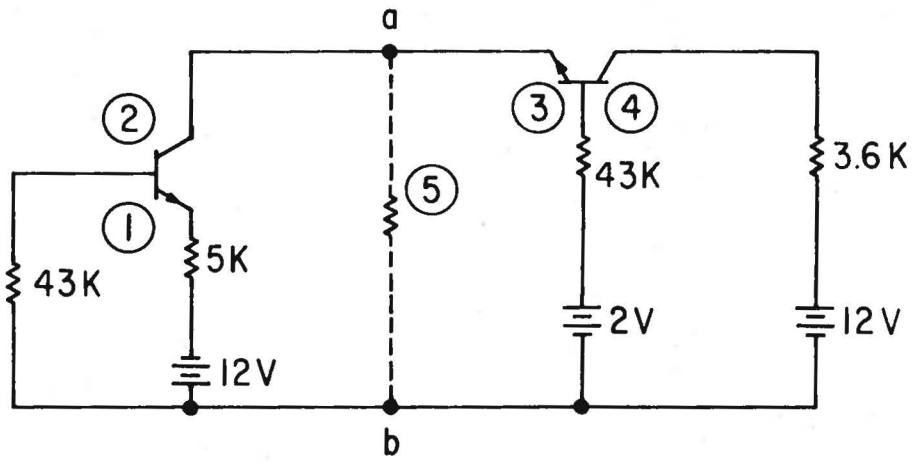


Fig. 9. Introduction of dummy ports to make the hybrid matrix sparse.

## A6. For Example 3 of Section VII

The hybrid matrix H is

| | | | | | | | | | | | | | | | | | | | | | | | |
|---|---|---|---|---|---|---|---|---|---|---|---|---|---|---|---|---|---|---|---|---|---|---|---|
| .1547E-02 | .1787E-01 | .1787E-01 | 0. | -.1941E-01 | .1941E-01 | 0. | .1941E-01 | 0. | 0. | -.1547E-02 | 0. | .1547E-02 | 0. | 0. | 0. | 0. | 0. | 0. | 0. | 0. | 0. | 0. | 0. |
| -.3094E-04 | .3606E-01 | .3606E-01 | 0. | -.3603E-01 | .3603E-01 | 0. | .3803E-01 | 0. | 0. | .3094E-04 | 0. | -.3094E-04 | 0. | 0. | 0. | 0. | 0. | 0. | 0. | 0. | 0. | 0. | 0. |
| -.1562E-02 | .2117E-01 | .2204E-01 | -.3124E-03 | -.2121E-01 | .2121E-01 | 0. | .2121E-01 | .1421E-03 | 0. | -.8450E-03 | 0. | -.6327E-03 | 0. | -.1238E-04 | 0. | 0. | .7175E-03 | -.1493E-04 | .2525E+00 | 0. | -.2525E-02 | | |
| 0. | 0. | -.9091E-03 | .9105E-03 | -.5011E-03 | .5011E-03 | 0. | .5011E-03 | .1429E-05 | 0. | -.1435E-02 | 0. | .1410E-02 | 0. | .2475E-04 | 0. | 0. | .1435E-02 | -.2986E-04 | -.5050E+00 | 0. | .5050E-02 | | |
| 0. | -.1941E-01 | -.2073E-01 | .7601E-03 | .2954E-01 | -.2950E-01 | .1414E-03 | -.2954E-01 | -.1400E-03 | .3380E-02 | .1435E-02 | .3300E-02 | -.8916E-02 | .2475E-04 | .4826E-04 | .7072E-03 | .9901E-04 | -.1435E-02 | .2986E-04 | -.5050E+00 | -.5000E+00 | -.4950E+00 | | |
| 0. | .3803E-03 | .4145E-03 | -.1520E-04 | -.5933E-03 | .5931E-01 | .2829E-03 | .5928E-03 | .2801E-05 | -.6601E-04 | -.2870E-04 | -.6601E-04 | .1783E-03 | -.4950E-06 | -.9851E-06 | -.1414E-04 | -.1980E-05 | .2870E-04 | -.5972E-06 | .1000E-01 | .1000E-01 | .9900E-02 | | |
| 0. | .1941E-01 | .2073E-01 | -.7601E-03 | -.2719E-01 | .2747E-01 | .2829E-03 | .2809E-01 | .1400E-03 | -.3300E-02 | -.1435E-02 | -.3300E-02 | .6401E-02 | .2420E-02 | -.4920E-04 | -.7072E-03 | -.9901E-04 | .1435E-02 | -.2900E-04 | .5000E+00 | .1000E+01 | .4950E+00 | | |
| 0. | .3383E-01 | .4145E-01 | -.1520E-02 | -.5933E-01 | .5961E-01 | .2831E-03 | .6113E-01 | .2801E-03 | -.6601E-02 | -.2870E-02 | -.6601E-02 | .1783E-01 | -.9951E-04 | -.9851E-04 | -.1414E-02 | -.1980E-03 | .2870E-02 | -.5972E-04 | .1000E+01 | .9900E+00 | .9901E-00 | | |
| 0. | 0. | 0. | .1429E-03 | .2475E-02 | -.2740E-02 | 0. | -.2475E-02 | .1429E-03 | 0. | 0. | 0. | -.2475E-02 | 0. | .2475E-02 | 0. | 0. | 0. | 0. | -.5000E+00 | 0. | .5050E+00 | | |
| -.1547E-02 | .1547E-02 | .1547E-02 | 0. | .8036E-02 | -.8036E-02 | 0. | -.8036E-02 | 0. | .6601E-02 | .2932E-02 | 0. | -.9507E-02 | 0. | 0. | 0. | 0. | -.1435E-02 | .2986E-04 | 0. | 0. | 0. | | |
| -.3094E-02 | .3094E-02 | .3094E-02 | 0. | .9405E-02 | -.9405E-02 | 0. | -.9405E-02 | 0. | .6535E-02 | .5964E-02 | 0. | -.1256E-01 | 0. | 0. | 0. | 0. | -.2870E-02 | .5972E-04 | 0. | 0. | 0. | | |
| .1547E-02 | -.1547E-02 | -.1547E-02 | 0. | -.2291E-02 | .2291E-02 | 0. | .2291E-02 | 0. | -.3300E-02 | -.2932E-02 | .3300E-02 | .3336E-02 | -.2475E-04 | -.2475E-04 | -.7072E-03 | -.9901E-04 | .1435E-02 | -.2900E-04 | 0. | .5000E+00 | .5000E+00 | | |
| .3094E-02 | -.3094E-02 | -.3094E-02 | 0. | -.1125E-01 | .1125E-01 | 0. | .1125E-01 | 0. | -.6601E-02 | -.5964E-02 | -.6601E-04 | .1434E-01 | -.4950E-04 | -.4950E-04 | -.1414E-02 | -.1980E-03 | .2870E-02 | -.5972E-04 | 0. | .1000E+01 | .1000E+01 | | |
| 0. | 0. | 0. | 0. | .2500E-02 | -.2500E-02 | 0. | -.2500E-02 | 0. | 0. | 0. | 0. | -.2500E-02 | .2500E-02 | 0. | 0. | 0. | 0. | 0. | 0. | -.5000E+00 | 0. | | |
| 0. | 0. | 0. | 0. | .2500E-02 | -.2500E-02 | 0. | -.2500E-02 | 0. | 0. | 0. | 0. | -.2500E-02 | 0. | .2500E-02 | 0. | 0. | 0. | 0. | 0. | 0. | -.5000E+00 | | |
| 0. | 0. | 0. | 0. | .1513E-02 | -.1513E-02 | 0. | -.1513E-02 | 0. | 0. | 0. | 0. | -.1513E-02 | 0. | 0. | .1414E-02 | .9902E+00 | 0. | 0. | 0. | 0. | 0. | | |
| 0. | 0. | 0. | 0. | .1598E-02 | -.1598E-02 | 0. | -.1598E-02 | 0. | 0. | 0. | 0. | -.1598E-02 | 0. | 0. | .1400E-02 | .1000E+01 | 0. | 0. | 0. | 0. | 0. | | |
| 0. | 0. | 0. | 0. | -.2840E-02 | .2840E-02 | 0. | .2840E-02 | 0. | 0. | -.2782E-02 | 0. | .2840E-02 | 0. | 0. | 0. | 0. | .2840E-02 | .3449E-03 | 0. | 0. | 0. | | |
| 0. | 0. | 0. | 0. | -.2782E-02 | .2782E-02 | 0. | .2782E-02 | 0. | 0. | -.2782E-02 | 0. | .2782E-02 | 0. | 0. | 0. | 0. | .2782E-02 | .7500E-03 | 0. | 0. | 0. | | |
| 0. | 0. | -.1000E+01 | .1000E+01 | .1000E+01 | -.1000E+01 | 0. | -.1000E+01 | 0. | 0. | 0. | 0. | 0. | 0. | 0. | 0. | 0. | 0. | 0. | 0. | 0. | 0. | | |
| 0. | 0. | 0. | 0. | .1000E+01 | -.1000E+01 | -.1000E+01 | 0. | 0. | 0. | 0. | 0. | -.1000E+01 | 0. | 0. | 0. | 0. | 0. | 0. | 0. | 0. | 0. | | |
| 0. | 0. | .1000E+01 | -.1000E+01 | 0. | 0. | 0. | 0. | -.1000E+01 | 0. | 0. | 0. | -.1000E+01 | 0. | 0. | 0. | 0. | 0. | 0. | 0. | 0. | 0. | | |

The source vector s is

| |
|---|
| .1520E+01 |
| .3120E+00 |
| .1601E+00 |
| .1100E-01 |
| -.2832E+00 |
| .5680E-03 |
| .2472E+00 |
| .5680E+00 |
| -.4000E-01 |
| -.1168E+00 |
| -.1288E+00 |
| .2368E-01 |
| .1536E+00 |
| -.4000E-01 |
| -.4009E-01 |
| -.2240E-01 |
| -.2240E-01 |
| .2568E-01 |
| .2800E-01 |
| 0. |
| 0. |
| 0. |